This article has been accepted for publication in a future issue of this journal, but has not been fully edited. Content may change prior to final publication. Citation information: DOI 10.1109/TVT.2018.2867894, IEEE Transactions on Vehicular Technology

Network-Coded Cooperative Spatial Multiplexing in Two-Way Relay Channels

Ali H. Bastami and Abolqasem Hessam

***Abstract*—In this paper, for a two-way relay channel (TWRC) comprising two multi-antenna transceivers and L single-antenna potential relay nodes, we propose three network-coded cooperative spatial multiplexing (CSM) schemes that effectively overcome the rate loss incurred due to the half-duplex limitation of the transceivers and the relay nodes and achieve high spectral efficiency. In the following, these three schemes are referred to as *time-division broadcast (TDBC)-CSM*, *incremental (I)-TDBC-CSM* and *multiple-access broadcast (MABC)-CSM*. We investigate these schemes in terms of the outage probability, the average transmission rate, the asymptotic behavior and the diversity-multiplexing tradeoff (DMT). The analysis of the paper shows that: (i) the I-TDBC-CSM scheme achieves the full diversity of order $L\min(M_1, M_2) + M_1M_2$, where M_1 and M_2 are the numbers of antennas employed by the two transceivers; (ii) the TDBC-CSM and MABC-CSM schemes achieve the diversity of order $L\min(M_1, M_2)$, where this quantity is the maximum achievable diversity gain in the absence of the direct link between the transceivers; (iii) the TDBC-CSM and I-TDBC-CSM schemes effectively overcome the rate loss incurred due to the half-duplex limitation of the relay nodes; (iv) the MABC-CSM scheme not only overcomes the half-duplex limitation of the relay nodes but also mitigates the spectral efficiency loss incurred due to the half-duplex limitation of the transceivers; and (v) if one or both of the transceivers are equipped with a massive antenna array, the asymptotic average rate of the CSM-based schemes scales linearly with the number of potential relay nodes, as opposed to the conventional relaying schemes in which the average rate is not scalable with L. We provide extensive simulation results to confirm the theoretical analysis of the paper. The simulation results show that for a given outage probability, the proposed schemes outperform the conventional relaying schemes in terms of the average transmission rate.**

***Index Terms*—Cooperative spatial multiplexing, incremental relaying, network coding, two-way relay channel (TWRC).**

I. Introduction

A. Background and Related Work

ONE of the main drawbacks of cooperative protocols is inefficient utilization of spectrum. This problem which is a consequence of the half-duplex limitation of the relay nodes can be alleviated by making use of the idea of incremental relaying [1]–[3]. In incremental relaying, the relay nodes help the source only if a failure occurs in the direct transmission. Typically, the success or failure of the direct transmission is determined based on either the decoding error [2] or the instantaneous received signal-to-noise ratio (SNR) [3] at the destination. Despite the fact that this technique achieves high spectral efficiency in the high-SNR regime, it has two main limitations: (i) its performance in the low and medium SNR regimes is not good enough; and (ii) the existence of a direct link between the source and the destination is required.

Cooperative spatial multiplexing (CSM) is another technique that effectively improves the bandwidth efficiency of half-duplex relaying by making use of the idea of spatial multiplexing in a distributed manner at the relay nodes [4]. In this technique, the source message is multiplexed onto multiple single-antenna relay nodes. As a result of the parallel transmissions of the relay nodes, a multiplexing gain is achieved and this leads to a high-rate flow of information from the source to the destination [4]–[9]. This technique has been widely investigated in the literature for the decode-and-forward (DF) [4], [5] and amplify-and-forward (AF) [6]–[9] relaying strategies.

The focus of [1]–[9] is on the unidirectional flow of information from the source to the destination. Usually in practice, instead of a source-destination pair, we have two transceivers that wish to exchange information with each other with the help of one or several relay nodes. In this network configuration, which is referred to as two-way relay channel (TWRC) [10], it is usually assumed that the transceivers and the relay nodes operate in the time-division duplex mode [10]–[32]. Under this assumption, if the two transceivers have the ability to communicate with each other directly without the help of the relay nodes, two time slots are sufficient for the exchange of two blocks of information symbols between the transceivers. However, in a TWRC, the number of required time slots typically varies from two to four depending on the protocol. Among the two-way relaying schemes, the four-time-slot scheme is the simplest one. However, the performance of this scheme is poor in terms of the spectral efficiency. The time-division broadcast (TDBC) scheme achieves higher spectral efficiency than the four-time-slot scheme by employing the idea of network coding [33] and reducing the number of required time slots to three [11]–[15]. The multiple-access broadcast (MABC) scheme further improves the spectral efficiency of the system by reducing the number of required time slots to two [16]–[20].

The incremental relaying technique can be coupled with the network coding operation to further enhance the spectral efficiency of the TWRC. Obviously, the idea of incremental relaying is not applicable to the MABC scheme due to the fact that the direct link cannot be exploited by the half-duplex transceivers. However, the TDBC scheme can benefit from this technique to achieve a higher spectral efficiency. This issue

The authors are with the Department of Electrical Engineering, K. N. Toosi University of Technology, Tehran 1631714191, Iran (e-mail: bastami@kntu.ac.ir, ahesam@mail.kntu.ac.ir).

This article has been accepted for publication in a future issue of this journal, but has not been fully edited. Content may change prior to final publication. Citation information: DOI 10.1109/TVT.2018.2867894, IEEE Transactions on Vehicular Technology

has been investigated in [21] and [22] for the DF and AF TWRCs, respectively. It has been shown that by employing the incremental relaying technique, the spectral efficiency of the TDBC scheme tends to that of the MABC scheme in the high-SNR regime, and at the same time, the TDBC scheme achieves a higher diversity gain compared with the MABC scheme [21], [22].

In contrast to the incremental relaying technique which is specific to the TDBC scheme, the spatial multiplexing technique is applicable to both the TDBC and MABC schemes. In the literature, this technique has been widely investigated for the MABC scenario [23]–[32]. In this network configuration which is usually referred to as multiple-input multiple-output (MIMO) TWRC, the spatial multiplexing is utilized in a centralized manner. Thus, it is necessary that the relay nodes are equipped with multiple antennas. In the literature, different issues related to the MIMO TWRC such as the design of precoder and decoder at the transceivers and the relay node [23]–[26], the design of physical-layer network coding (PNC) [27], [28], the antenna selection at the relay node [29], [30], and the best relay selection in the multi-relay scenario [31], [32], have been investigated for the single-relay DF [23], [27]–[29], single-relay AF [24]–[26], [30] and multi-relay AF [31], [32] networks. In [34], for a multi-user MIMO system, a space-time coded linear PNC scheme has been designed that guarantees the full-diversity and full-rate transmission. This PNC scheme can be applied to various system models such as the MIMO TWRC and the MIMO multiple-access relay network.

B. Motivation and Contributions of the Paper

Usually in practice, the relay nodes are simple terminals that cannot support multiple antennas due to size or other practical limitations. For example, consider a wireless network in which the mobile users that are idle act as relays. Typically, these terminals are not able to support multiple antennas, or at least, the number of antennas cannot be large. Under these circumstances, the centralized version of spatial multiplexing cannot be utilized efficiently at the relay node to achieve high spectral efficiency. The CSM technique can overcome this limitation by employing single-antenna terminals in a distributed manner. To the best of our knowledge, the CSM technique has not been investigated in the literature for two-way relaying, and this motivates our work. The aim of the present paper is to propose and analyze spectrally efficient protocols for the network-coded TWRC based on the CSM technique. The main contributions of this paper can be summarized as follows.

- In this paper, for a TWRC comprising two multi-antenna transceivers and L single-antenna DF relay nodes, we propose three network-coded CSM schemes that effectively overcome the rate loss incurred due to the half-duplex limitation of the transceivers and the relay nodes and achieve high spectral efficiency. In the following, these three schemes are referred to as *TDBC-CSM*, *incremental (I)-TDBC-CSM* and *MABC-CSM*.
- We analyze the performance of these schemes in terms of the outage probability, the asymptotic behavior and the diversity-multiplexing tradeoff (DMT) over identically and non-identically distributed Rayleigh fading channels. The outage probability reflects the rate of unsuccessful information exchange between the transceivers, and the diversity order determines how fast the outage probability decays with increasing SNR. The asymptotic analysis of the outage probability shows that for a fixed target rate:
  1) The I-TDBC-CSM scheme achieves the full diversity of order $L\min(M_1, M_2) + M_1M_2$, where M_1 and M_2 are the numbers of antennas employed by the two transceivers and L is the number of potential relay nodes.
  2) The TDBC-CSM and MABC-CSM schemes achieve the diversity of order $L\min(M_1, M_2)$, where this quantity is the maximum achievable diversity gain in the absence of the direct link between the transceivers.
- The proposed schemes belong to the category of variable-rate protocols. To characterize the bandwidth efficiency of these schemes, we analyze their performance in terms of the average transmission rate. The analysis of the paper shows that:
  1) As L increases, the asymptotic average rate of the TDBC-CSM scheme tends to that of the case that two half-duplex transceivers directly exchange information with each other. This implies that the TDBC-CSM scheme effectively overcomes the rate loss incurred due to the half-duplex limitation of the relay nodes.
  2) The asymptotic average rate of the I-TDBC-CSM scheme equals that of the direct transmission scheme irrespective of the number of potential relay nodes. This observation reveals that the I-TDBC-CSM scheme effectively overcomes the half-duplex limitation of the relay nodes even when L is small.
  3) With increasing the number of potential relay nodes, the MABC-CSM scheme asymptotically behaves similar to the case that two full-duplex transceivers directly exchange information with each other. This implies that the MABC-CSM scheme not only overcomes the half-duplex limitation of the relay nodes but also mitigates the spectral efficiency loss incurred due to the half-duplex limitation of the transceivers.
  4) If one or both of the transceivers are equipped with a massive antenna array, the asymptotic average rate of the CSM-based schemes scales linearly with the number of potential relay nodes, as opposed to the conventional relaying schemes in which the average rate is not scalable with L.
- We provide extensive simulation results to confirm the theoretical analysis of the paper. The simulation results show that for a given outage probability, the CSM-based schemes outperform the conventional relaying schemes in terms of the average transmission rate over the entire range of SNR. These observations imply that the CSM-based schemes are suitable candidates for reliable high data rate communications.

This article has been accepted for publication in a future issue of this journal, but has not been fully edited. Content may change prior to final publication. Citation information: DOI 10.1109/TVT.2018.2867894, IEEE Transactions on Vehicular Technology

C. Outline of the Paper

The remainder of this paper is organized as follows. Section II introduces the proposed schemes. Sections III analyzes the outage probability performance of the proposed schemes. Section IV investigates the proposed schemes in terms of the average transmission rate. Section V studies the asymptotic behavior of the outage probability and derives the DMT expressions. Section VI provides some simulation results and numerical examples. Finally, Section VII summarizes the main results of the paper.

Notation: We use boldface lowercase and uppercase letters for vectors and matrices, respectively. For the vector $\mathbf{x}$, $\mathbf{x}^{tr}$ and $\|\mathbf{x}\|$ denote the transpose and the norm of $\mathbf{x}$. For the matrix $\mathbf{X}$, $\mathbf{X}^H$, $\det(\mathbf{X})$ and $\|\mathbf{X}\|_F$ denote the conjugate transpose, the determinant and the Frobenius norm of $\mathbf{X}$, respectively. $\mathbf{I}_M$ denotes the $M \times M$ identity matrix. $\mathbf{0}_{M\times N}$ denotes an $M \times N$ all-zero matrix. For a set $\mathcal{X}$, $|\mathcal{X}|$ denotes the cardinality of $\mathcal{X}$. $\mathbb{C}$ denotes the set of complex numbers. $\mathbb{N}$ denotes the set of natural numbers, i.e. nonnegative integers. $\lceil x \rceil$ denotes the smallest integer greater than or equal to x. x^+ denotes $\max(0, x)$. $\mathbb{E}\{.\}$ denotes the expectation operator. We use $\mathbb{P}(.)$ to denote the probability of the given event. For a random variable X, $f_X(x)$ denotes the probability density function (PDF) of X. We use $X \sim \mathrm{Gamma}(t_1, t_2)$ to denote that X is a gamma random variable with parameters t_1 and t_2, i.e. $f_X(x) = \frac{x^{t_1-1}}{t_2^{t_1}\Gamma(t_1)} e^{-x/t_2}$, $x > 0$. $\Gamma(t) = \int_0^\infty x^{t-1}e^{-x}dx$ is the complete gamma function and $\Gamma(t_1, t_2) = \int_{t_2}^\infty x^{t_1-1}e^{-x}dx$ is the upper incomplete gamma function. We use $G_1(x) \sim G_2(x)$ to denote that the functions $G_1(x)$ and $G_2(x)$ are asymptotically equivalent, i.e. $G_1(x)/G_2(x) \to 1$ as $x \to \infty$.

II. System Model and Protocol Description

A. General Assumptions

We consider a TWRC comprising two transceivers, denoted by T_1 and T_2, and a set of potential relay nodes, denoted by $\mathcal{P} = \{1, \ldots, L\}$, as shown in Fig. 1. The transceivers T_1 and T_2 are equipped with M_1 and M_2 antennas, respectively, and the relay nodes are single-antenna terminals. All the nodes transmit over the same frequency band and operate in a half-duplex mode. All the links are assumed to be independent of each other and are subject to frequency non-selective Rayleigh fading and additive white Gaussian noise (AWGN). It is assumed that the fading channel varies slowly such that it can be assumed almost constant over each period of $N\max(M_1, M_2)$ symbol intervals, where N is chosen based on the channel coherence time. Regarding the availability of the direct link between T_1 and T_2, we make the following assumptions:

- In our TDBC-based schemes, we consider the following two cases: (i) The case that the direct link does not exist between T_1 and T_2 (e.g. due to shadowing or severe path loss). This scheme is referred to as TDBC-CSM. (ii) The case that the direct link exists. In this case, to make use of spectrum as efficiently as possible, the relay nodes cooperate incrementally. This scheme is referred to as I-TDBC-CSM.

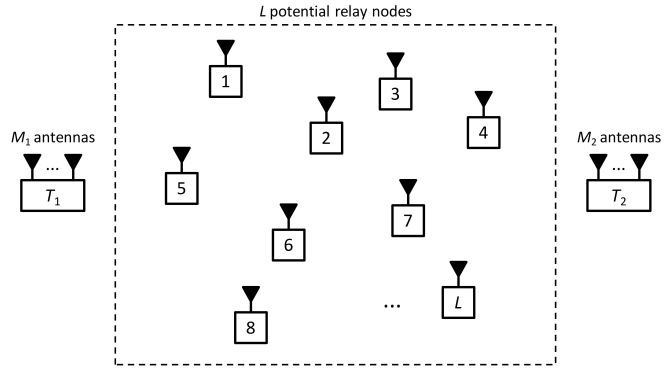

Fig. 1. System model: A TWRC comprising two transceivers T_1 and T_2, and L potential relay nodes, denoted by $1, \ldots, L$.

- In our MABC-based scheme, due to the half-duplex limitation of T_1 and T_2 and the fact that the two transceivers simultaneously transmit in the multiple-access phase, the direct link cannot be exploited, regardless of the fact that this link is physically available or not. This scheme is referred to as MABC-CSM.

B. TDBC-CSM Scheme

In time slots 1 and 2, T_1 and T_2 broadcast their messages to the relay nodes, respectively. The received signals at relay ℓ during the first two time slots, i.e. for $n = 1, \ldots, N$, and $n = N+1, \ldots, 2N$, can be written as

$$y_\ell(n) = \sqrt{\frac{E_{T_1}}{M_1}}\, \mathbf{h}_{T_1,\ell}^{tr}\, \mathbf{s}_1(n) + z_\ell(n),\ n = 1, \ldots, N \tag{1}$$

$$y_\ell(n) = \sqrt{\frac{E_{T_2}}{M_2}}\, \mathbf{h}_{T_2,\ell}^{tr}\, \mathbf{s}_2(n) + z_\ell(n),\ n = N+1, \ldots, 2N \tag{2}$$

where $y_\ell(n)$ denotes the received signal at relay ℓ at time index n, E_{T_i} is the average energy transmitted by T_i over a symbol period, $\mathbf{h}_{T_i,\ell} \in \mathbb{C}^{M_i}$ denotes the MISO channel from T_i to relay ℓ, $\mathbf{s}_i(n) \in \mathbb{C}^{M_i}$ is the information-bearing signal transmitted by T_i, where $\mathbb{E}\{\mathbf{s}_i(n)\mathbf{s}_i^H(n)\} = \mathbf{I}_{M_i}$, and $z_\ell(n)$ is the AWGN process at relay ℓ and is independent and identically distributed (i.i.d.) over time with distribution $\mathcal{CN}(0, N_0)$, where $i = 1, 2$ and $\ell = 1, \ldots, L$. Under Rayleigh fading assumption, each entry of $\mathbf{h}_{T_i,\ell}$ is a zero mean circularly symmetric complex Gaussian random variable with variance $\sigma^2_{T_i,\ell}$. This variance is proportional to $d^{-v}_{T_i,\ell}$, where $d_{T_i,\ell}$ denotes the distance between T_i and relay ℓ and v is the path-loss exponent.

Let us define the set of reliable relay nodes $\mathcal{C}$ as the set of relay nodes that can decode $\mathbf{s}_1(n)$ and $\mathbf{s}_2(n)$ successfully. Let R denote the target rate for the transmission of information in the network. For the desired rate R, the set $\mathcal{C}$ can be described as

$$\mathcal{C} = \{\ell \in \mathcal{P} \mid I_{T_1,\ell} \geq R,\, I_{T_2,\ell} \geq R\} \tag{3}$$

where $I_{T_i,\ell}$ is the achievable rate for the link from T_i to relay ℓ conditioned on the channel vector $\mathbf{h}_{T_i,\ell}$, which is given by

$$I_{T_i,\ell} = \log_2\left(1 + \frac{E_{T_i}}{M_i N_0}\|\mathbf{h}_{T_i,\ell}\|^2\right), \quad i = 1, 2. \tag{4}$$

This article has been accepted for publication in a future issue of this journal, but has not been fully edited. Content may change prior to final publication. Citation information: DOI 10.1109/TVT.2018.2867894, IEEE Transactions on Vehicular Technology

Each of the relay nodes belonging to the set $\mathcal{C}$ performs the following three steps independent of other relay nodes: (i) decodes $\mathbf{s}_1(n)$ and $\mathbf{s}_2(n)$ and obtains two bit streams corresponding to these two signals, (ii) combines these two bit streams using the conventional bitwise XOR-based network coding operation [12], and (iii) re-encodes and remodulates the network-coded bit stream to obtain the sequence of symbols $s_{\rm NC}(1), \ldots, s_{\rm NC}(N\max(M_1, M_2))$.

At the beginning of the broadcast phase, the relay nodes sequentially inform the transceivers whether they belong to the set $\mathcal{C}$ or not by broadcasting a positive or negative acknowledgement. Let $\mathcal{C} = \{\ell_1, \ldots, \ell_{\theta_\mathcal{C}}\}$, where $\ell_1 < \cdots < \ell_{\theta_\mathcal{C}}$ and $\theta_\mathcal{C} = |\mathcal{C}|$. In response to relay $\ell_j \in \mathcal{C}$, $j = 1, ..., \theta_\mathcal{C}$, one of the transceivers, for example T_1, sends back the ordering index j based on which the reliable relay nodes become aware of the multiplexing pattern. After that, the reliable relay nodes simultaneously broadcast the spatially multiplexed signal to the destination nodes. The received signals at T_1 and T_2 during the broadcast phase can be described as

$$\mathbf{y}_{T_i}(n) = \sqrt{E/\theta_\mathcal{C}}\,\mathbf{H}_{\mathcal{C},T_i}\,\mathbf{s}_\mathcal{C}(n) + \mathbf{z}_{T_i}(n), \quad i = 1, 2 \tag{5}$$

where $n = 2N+1, \ldots, 2N + \lceil N\max(M_1, M_2)/\theta_\mathcal{C}\rceil$, $\mathbf{y}_{T_i}(n) \in \mathbb{C}^{M_i}$ is the received vector by T_i, E is the total average energy allocated to the relay nodes, $\mathbf{H}_{\mathcal{C},T_i} \in \mathbb{C}^{M_i \times \theta_\mathcal{C}}$ denotes the distributed MIMO channel matrix from $\mathcal{C}$ to T_i, $\mathbf{z}_{T_i}(n) \sim \mathcal{CN}(\mathbf{0}_{M_i\times 1}, N_0\mathbf{I}_{M_i})$ is the AWGN process at T_i and is i.i.d. over time, and $\mathbf{s}_\mathcal{C}(n)$ is a $\theta_\mathcal{C} \times 1$ vector whose jth element is the transmitted symbol by relay $\ell_j \in \mathcal{C}$ at time index n. The jth element of $\mathbf{s}_\mathcal{C}(n)$ is constructed by relay ℓ_j based on the multiplexing pattern as $s_{\rm NC}\left((n-2N-1)\theta_\mathcal{C} + j\right)$, $j = 1, \ldots, \theta_\mathcal{C}$.

Finally, T_1 and T_2 perform detection based on $\mathbf{y}_{T_1}(n)$ and $\mathbf{y}_{T_2}(n)$, respectively, and then cancel the self-interference caused by the network coding operation to obtain their intended symbols.

C. I-TDBC-CSM Scheme

In time slot 1, T_1 broadcasts its information-bearing signal and the relay nodes and the opposite transceiver listen. Similarly, in time slot 2, T_2 broadcasts its signal and all the other nodes listen. The received signals by the transceivers during the first two time slots can be expressed as

$$\mathbf{y}_{T_2}(n) = \sqrt{\frac{E_{T_1}}{M_1}}\,\mathbf{H}_{T_1,T_2}\,\mathbf{s}_1(n) + \mathbf{z}_{T_2}(n), \;\; n = 1, \ldots, N \tag{6}$$

$$\mathbf{y}_{T_1}(n) = \sqrt{\frac{E_{T_2}}{M_2}}\,\mathbf{H}_{T_2,T_1}\,\mathbf{s}_2(n) + \mathbf{z}_{T_1}(n), \;\; n = N+1, \ldots, 2N \tag{7}$$

where $\mathbf{y}_{T_i}(n) \in \mathbb{C}^{M_i}$ is the received vector by T_i, $\mathbf{H}_{T_k,T_i} \in \mathbb{C}^{M_i \times M_k}$ denotes the channel matrix for the T_k-T_i MIMO link and $\mathbf{z}_{T_i}(n)$ is the AWGN process at T_i with distribution $\mathcal{CN}(\mathbf{0}_{M_i\times 1}, N_0\mathbf{I}_{M_i})$, where $i, k = 1, 2$ and $i \neq k$. The received signals at relay ℓ during the first two time slots are given in (1) and (2).

Let I_{T_1,T_2} and I_{T_2,T_1} denote the achievable rates for the T_1-T_2 and T_2-T_1 links conditioned on the channel matrices $\mathbf{H}_{T_1,T_2}$ and $\mathbf{H}_{T_2,T_1}$, respectively, i.e.

$$I_{T_k,T_i} = \log_2\det\left(\mathbf{I}_{M_i} + \frac{E_{T_k}}{M_k N_0}\mathbf{H}_{T_k,T_i}\mathbf{H}_{T_k,T_i}^H\right) \tag{8}$$

where $i, k = 1, 2$, $i \neq k$. Based on I_{T_1,T_2} and I_{T_2,T_1}, one of the following modes of operation takes place:

Mode 1: $I_{T_1,T_2} \geq R$ and $I_{T_2,T_1} \geq R$. In this mode, both of the direct links are reliable. Thus, T_1 and T_2 rely on the direct signals and the cooperation phase is skipped.

Mode 2: $I_{T_1,T_2} \geq R$ and $I_{T_2,T_1} < R$. In this mode, only the link from T_1 to T_2 is reliable. Thus, in the third time slot, the reliable relay nodes decode, re-encode and forward the signal received from T_2 to T_1 by employing the CSM technique in a similar way as in the broadcast phase of the TDBC-CSM scheme described in Section II-B. The set of reliable relay nodes consists of those relay nodes that decode $\mathbf{s}_2(n)$ successfully, i.e.

$$\mathcal{C} = \{\ell \in \mathcal{P} \,|\, I_{T_2,\ell} \geq R\} \tag{9}$$

where $I_{T_2,\ell}$ is given in (4). In this mode, T_1 performs detection based on the relayed signal and T_2 relies on the direct signal.

Mode 3: $I_{T_1,T_2} < R$ and $I_{T_2,T_1} \geq R$. In this mode, only the link from T_2 to T_1 is reliable. Thus, in the third time slot, the reliable relay nodes decode, re-encode and forward the signal received from T_1 to T_2 by employing the CSM technique in a similar way as in the broadcast phase of the TDBC-CSM scheme. The set of reliable relay nodes comprises those relay nodes that decode $\mathbf{s}_1(n)$ successfully, i.e.

$$\mathcal{C} = \{\ell \in \mathcal{P} \,|\, I_{T_1,\ell} \geq R\} \tag{10}$$

where $I_{T_1,\ell}$ is given in (4). In this mode, T_2 performs detection based on the relayed signal and T_1 relies on the direct signal.

Mode 4: $I_{T_1,T_2} < R$ and $I_{T_2,T_1} < R$. In this mode, both of the direct links are unreliable. Thus, in the third time slot, the reliable relay nodes broadcast the network-coded signal to T_1 and T_2 by employing the CSM technique in the same way as in the broadcast phase of the TDBC-CSM scheme. In this mode, T_1 and T_2 perform detection based on the relayed signal.

An expression similar to (5) can be written for the received signal at the destination corresponding to modes 2–4.

Obviously, in this scheme, the relay nodes need to be aware of the mode of operation. This information can be easily made available to the relay nodes by broadcasting a positive or negative acknowledgement by T_1 and T_2 at the end of the first and second time slots.

D. MABC-CSM Scheme

In this scheme, during the first time slot, T_1 and T_2 simultaneously transmit their signals to the relay nodes. The received signal at relay ℓ can be expressed as

$$y_\ell(n) = \sqrt{\frac{E_{T_1}}{M_1}}\,\mathbf{h}_{T_1,\ell}^{tr}\,\mathbf{s}_1(n) + \sqrt{\frac{E_{T_2}}{M_2}}\,\mathbf{h}_{T_2,\ell}^{tr}\,\mathbf{s}_2(n) + z_\ell(n) \tag{11}$$

where $n = 1, \ldots, N$ and $\ell = 1, \ldots, L$. Whether or not relay ℓ belongs to the set of reliable relay nodes depends on the detection technique employed by the relay nodes. In the case of joint detection, each relay node, independent of

This article has been accepted for publication in a future issue of this journal, but has not been fully edited. Content may change prior to final publication. Citation information: DOI 10.1109/TVT.2018.2867894, IEEE Transactions on Vehicular Technology

other relay nodes, simultaneously recovers $\mathbf{s}_1(n)$ and $\mathbf{s}_2(n)$ from the superimposed signal $y_\ell(n)$ using the maximum likelihood (ML) detection technique. Let $R_{T_i,\ell}$ denote the rate for the link from T_i to relay ℓ, where $i = 1, 2$. Under the assumption of joint detection, only those $(R_{T_1,\ell}, R_{T_2,\ell})$ pairs are achievable that satisfy the following three inequalities [35]:

$$\begin{aligned} R_{T_1,\ell} &\le \log_2\left(1+\frac{E_{T_1}}{M_1 N_0}\|\mathbf{h}_{T_1,\ell}\|^2\right) \triangleq {}_1I_\ell \\ R_{T_2,\ell} &\le \log_2\left(1+\frac{E_{T_2}}{M_2 N_0}\|\mathbf{h}_{T_2,\ell}\|^2\right) \triangleq {}_2I_\ell \\ \sum_{i=1}^{2} R_{T_i,\ell} &\le \log_2\left(1+\frac{E_{T_1}}{M_1 N_0}\|\mathbf{h}_{T_1,\ell}\|^2+\frac{E_{T_2}}{M_2 N_0}\|\mathbf{h}_{T_2,\ell}\|^2\right) \triangleq {}_3I_\ell \end{aligned} \tag{12}$$

Accordingly, for the target rate R, the set of reliable relay nodes $\mathcal{C}$ (that can reliably decode $\mathbf{s}_1(n)$ and $\mathbf{s}_2(n)$) can be described as

$$\mathcal{C} = \{\ell \in \mathcal{P} \,|\, {}_1I_\ell \ge R,\, {}_2I_\ell \ge R,\, {}_3I_\ell \ge 2R\}. \tag{13}$$

This set contains those relay nodes whose achievable rate regions include the rate pair (R, R).

The broadcast phase of the protocol is the same as that of the TDBC-CSM scheme. In this phase, each of the reliable relay nodes combines the two decoded signals using the network coding operation, re-encodes the network-coded signal and broadcasts the resulting signal back to both transceivers by employing the CSM technique as described in Section II-B.

III. Outage Probability Analysis

We say that the exchange of information between T_1 and T_2 undergoes an outage state if the desired rate cannot be satisfied for T_1 and/or T_2. In this section, we investigate the performance of the proposed schemes in terms of the outage probability over Rayleigh fading channel.

A. TDBC-CSM Scheme

Let $I_{\mathcal{C},T_i}$ denote the achievable rate for the MIMO link from $\mathcal{C}$ to T_i. Based on the aforementioned definition, an outage state occurs if either of the following events takes place: (i) $\mathcal{E}_1 = \{I_{\mathcal{C},T_1} < R,\, I_{\mathcal{C},T_2} \ge R\}$, (ii) $\mathcal{E}_2 = \{I_{\mathcal{C},T_1} \ge R,\, I_{\mathcal{C},T_2} < R\}$, and (iii) $\mathcal{E}_3 = \{I_{\mathcal{C},T_1} < R,\, I_{\mathcal{C},T_2} < R\}$. Accordingly, the outage probability conditioned on the set of reliable relay nodes $\mathcal{C}$ can be computed as

$$P_{\text{out}|\mathcal{C}}^{\text{TDBC-CSM}}(R) = 1 - \mathbb{P}(I_{\mathcal{C},T_1} \ge R)\,\mathbb{P}(I_{\mathcal{C},T_2} \ge R). \tag{14}$$

Obviously, for the case that $\mathcal{C}$ is empty, we have $I_{\mathcal{C},T_1} = I_{\mathcal{C},T_2} = 0$. In this case, the outage probability equals 1, i.e.

$$P_{\text{out}|\mathcal{C}=\emptyset}^{\text{TDBC-CSM}}(R) = 1. \tag{15}$$

Let us focus on the case that the set of reliable relay nodes is nonempty. Based on (5), $I_{\mathcal{C},T_1}$ and $I_{\mathcal{C},T_2}$ conditioned on the channel matrices $\mathbf{H}_{\mathcal{C},T_1}$ and $\mathbf{H}_{\mathcal{C},T_2}$ can be expressed as

$$I_{\mathcal{C},T_i} = \mu_{\mathcal{C}} \log_2 \det\left(\mathbf{I}_{M_i} + \frac{E}{\theta_{\mathcal{C}} N_0}\mathbf{H}_{\mathcal{C},T_i}\mathbf{H}_{\mathcal{C},T_i}^H\right), \quad i = 1, 2 \tag{16}$$

where the scaling factor $\mu_{\mathcal{C}}$ is due to the fact that the duration of the broadcast phase of the protocol is $\mu_{\mathcal{C}}$ times that of the first two time slots, where $\mu_{\mathcal{C}} = \frac{\lceil N\max(M_1,M_2)/\theta_{\mathcal{C}}\rceil}{N}$. Let $q = \lceil N\max(M_1,M_2)/\theta_{\mathcal{C}}\rceil - N\max(M_1,M_2)/\theta_{\mathcal{C}}$. Thus, $\mu_{\mathcal{C}}$ can be rewritten as $\mu_{\mathcal{C}} = (N\max(M_1,M_2) + q\theta_{\mathcal{C}})/N\theta_{\mathcal{C}}$. Noting the fact that $\theta_{\mathcal{C}} \le L \ll N$ (e.g. we have $L = 5$ and $N = 10^4$)[1] and that $0 \le q < 1$, $\mu_{\mathcal{C}}$ can be well approximated as $\mu_{\mathcal{C}} = \max(M_1, M_2)/\theta_{\mathcal{C}}$. Substituting (16) into (14) and using Jensen's approximation, we obtain

$$P_{\text{out}|\mathcal{C}\neq\emptyset}^{\text{TDBC-CSM}}(R) \approx 1 - \prod_{i=1}^{2}\mathbb{P}\left(\frac{E}{\theta_{\mathcal{C}} N_0}\|\mathbf{H}_{\mathcal{C},T_i}\|_F^2 \ge \psi_{\mathcal{C},i}\right) \tag{17}$$

where $\psi_{\mathcal{C},i} = \left(2^{R/\mu_{\mathcal{C}}\delta_i} - 1\right)\delta_i$, and $\delta_i = \min(M_i, \theta_{\mathcal{C}})$. Under Rayleigh fading assumption, each entry of the j-th column of $\mathbf{H}_{\mathcal{C},T_i}$ is a zero mean circularly symmetric complex Gaussian random variable with variance $\sigma^2_{\ell_j,T_i}$. Since in general, the relay nodes are in different locations, the variances $\sigma^2_{\ell_j,T_i}$, $1 \le j \le \theta_{\mathcal{C}}$, are not necessarily identical. Thus in general, $\|\mathbf{H}_{\mathcal{C},T_i}\|_F^2$ is not a Gamma random variable. Let $X_i \triangleq \frac{E}{\theta_{\mathcal{C}} N_0}\|\mathbf{H}_{\mathcal{C},T_i}\|_F^2$. For arbitrary values of the variances $\sigma^2_{\ell_j,T_i}$, $1 \le j \le \theta_{\mathcal{C}}$, the PDF of X_i can be shown to be [37]

$$f_{X_i}(x) = \sum_{k=0}^{K} \frac{\alpha_{k,i}}{\bar{\gamma}_{\min,i}^{\theta_{\mathcal{C}}M_i+k}\,\Gamma(\theta_{\mathcal{C}}M_i + k)} x^{\theta_{\mathcal{C}}M_i+k-1} e^{-x/\bar{\gamma}_{\min,i}} \tag{18}$$

where $\bar{\gamma}_{\min,i}$ and $\alpha_{k,i}$ are given by

$$\bar{\gamma}_{\min,i} = \min_{1\le j\le\theta_{\mathcal{C}}} \overline{\gamma}_{\ell_j,T_i} \tag{19}$$

$$\alpha_{k,i} = \beta_{k,i}\left(\prod_{j=1}^{\theta_{\mathcal{C}}} \frac{\bar{\gamma}_{\min,i}}{\overline{\gamma}_{\ell_j,T_i}}\right)^{M_i} \tag{20}$$

where $\overline{\gamma}_{\ell_j,T_i} = E\sigma^2_{\ell_j,T_i}/\theta_{\mathcal{C}}N_0$ is the average SNR per antenna at T_i received from relay ℓ_j, and $\beta_{k,i}$ is computed recursively as

$$\beta_{k+1,i} = \frac{1}{k+1}\sum_{t=1}^{k+1} t\,\lambda_{t,i}\,\beta_{k+1-t,i}, \;\; k \in \mathbb{N} \tag{21}$$

where $\beta_{0,i} = 1$ and $\lambda_{t,i}$ is given by

$$\lambda_{t,i} = \frac{M_i}{t}\sum_{j=1}^{\theta_{\mathcal{C}}}\left(1 - \frac{\bar{\gamma}_{\min,i}}{\overline{\gamma}_{\ell_j,T_i}}\right)^t. \tag{22}$$

Setting $K = \infty$ in (18) yields an exact expression for $f_{X_i}(x)$. However, in practice, a small finite value of K results in an accurate expression for the PDF. Using (18), the probability of the event $X_i \ge \psi_{\mathcal{C},i}$ can be obtained as

$$\mathbb{P}(X_i \ge \psi_{\mathcal{C},i}) = \sum_{k=0}^{K}\alpha_{k,i}\frac{\Gamma(\theta_{\mathcal{C}}M_i + k,\, \psi_{\mathcal{C},i}/\bar{\gamma}_{\min,i})}{\Gamma(\theta_{\mathcal{C}}M_i + k)}. \tag{23}$$

[1]For example, in LTE-A, the subframe duration is 1 ms [36]. Assuming the data rate of 10 MHz, which is less than the typical data rates in current wireless standards, we conclude that the value of N is at least 10^4.

This article has been accepted for publication in a future issue of this journal, but has not been fully edited. Content may change prior to final publication. Citation information: DOI 10.1109/TVT.2018.2867894, IEEE Transactions on Vehicular Technology

$$P_{\text{out}}^{\text{TDBC-CSM}}(R) \approx \prod_{j\in\mathcal{P}}\left(1-\frac{\Gamma\left(M_1,\frac{2^R-1}{\overline{\gamma}_{T_1,j}}\right)}{\Gamma(M_1)}\times\frac{\Gamma\left(M_2,\frac{2^R-1}{\overline{\gamma}_{T_2,j}}\right)}{\Gamma(M_2)}\right)+\sum_{\mathcal{C}\neq\emptyset}\left\{\left(1-\prod_{i=1}^{2}\sum_{k=0}^{K}\alpha_{k,i}\frac{\Gamma\left(\theta_{\mathcal{C}}M_i+k\,,\,\frac{\psi_{\mathcal{C},i}}{\overline{\gamma}_{\min,i}}\right)}{\Gamma\left(\theta_{\mathcal{C}}M_i+k\right)}\right)\right.$$
$$\left.\times\prod_{\ell\in\mathcal{C}}\left(\frac{\Gamma\left(M_1,\frac{2^R-1}{\overline{\gamma}_{T_1,\ell}}\right)}{\Gamma(M_1)}\times\frac{\Gamma\left(M_2,\frac{2^R-1}{\overline{\gamma}_{T_2,\ell}}\right)}{\Gamma(M_2)}\right)\prod_{j\notin\mathcal{C}}\left(1-\frac{\Gamma\left(M_1,\frac{2^R-1}{\overline{\gamma}_{T_1,j}}\right)}{\Gamma(M_1)}\times\frac{\Gamma\left(M_2,\frac{2^R-1}{\overline{\gamma}_{T_2,j}}\right)}{\Gamma(M_2)}\right)\right\} \quad (27)$$

Substituting (23) into (17), the outage probability conditioned on the nonempty set $\mathcal{C}$ can be written as

$$P_{\text{out}|\mathcal{C}\neq\emptyset}^{\text{TDBC-CSM}}(R)\approx 1-\prod_{i=1}^{2}\sum_{k=0}^{K}\alpha_{k,i}\frac{\Gamma\left(\theta_{\mathcal{C}}M_i+k\,,\,\psi_{\mathcal{C},i}/\overline{\gamma}_{\min,i}\right)}{\Gamma\left(\theta_{\mathcal{C}}M_i+k\right)}. \quad (24)$$

Averaging $P_{\text{out}|\mathcal{C}}^{\text{TDBC-CSM}}(R)$ over $\mathcal{C}$, the unconditional outage probability can be calculated as

$$P_{\text{out}}^{\text{TDBC-CSM}}(R)=\sum_{\mathcal{C}}P_{\text{out}|\mathcal{C}}^{\text{TDBC-CSM}}(R)\,\mathbb{P}\left(\mathcal{C}\right) \quad (25)$$

where $P_{\text{out}|\mathcal{C}}^{\text{TDBC-CSM}}(R)$ is given in (15) and (24) for the cases $\mathcal{C}=\emptyset$ and $\mathcal{C}\neq\emptyset$, respectively, and $\mathbb{P}\left(\mathcal{C}\right)$ is the probability mass function (PMF) of the set $\mathcal{C}$, which is given by

$$\mathbb{P}\left(\mathcal{C}\right)=\prod_{\ell\in\mathcal{C}}\left(\frac{\Gamma\left(M_1,\frac{2^R-1}{\overline{\gamma}_{T_1,\ell}}\right)}{\Gamma(M_1)}\times\frac{\Gamma\left(M_2,\frac{2^R-1}{\overline{\gamma}_{T_2,\ell}}\right)}{\Gamma(M_2)}\right)\times\prod_{j\notin\mathcal{C}}\left(1-\frac{\Gamma\left(M_1,\frac{2^R-1}{\overline{\gamma}_{T_1,j}}\right)}{\Gamma(M_1)}\times\frac{\Gamma\left(M_2,\frac{2^R-1}{\overline{\gamma}_{T_2,j}}\right)}{\Gamma(M_2)}\right) \quad (26)$$

where $\overline{\gamma}_{T_i,\ell}=E_{T_i}\sigma_{T_i,\ell}^2/M_iN_0$ is the mean value of $\gamma_{T_i,\ell}=E_{T_i}\|\mathbf{h}_{T_i,\ell}\|^2/M_iN_0$, where $\gamma_{T_i,\ell}$ is the instantaneous received SNR at relay ℓ from T_i, $i=1,2$. The derivation of (26) is given in Appendix A. Substituting (15), (24) and (26) into (25), the outage probability for the TDBC-CSM scheme is obtained in closed form as (27), shown at the top of the page.

B. I-TDBC-CSM Scheme

Let $P_{\text{out}|\text{mode }m}^{\text{I-TDBC-CSM}}(R)$ denote the conditional outage probability corresponding to the case that the system operates in mode m. Based on the total probability theorem, the outage probability can be computed as

$$P_{\text{out}}^{\text{I-TDBC-CSM}}(R)=\sum_{m=1}^{4}P_{\text{out}|\text{mode }m}^{\text{I-TDBC-CSM}}(R)\,\mathbb{P}(\text{mode }m). \quad (28)$$

In the following, we compute $P_{\text{out}|\text{mode }m}^{\text{I-TDBC-CSM}}(R)$ and $\mathbb{P}(\text{mode }m)$ corresponding to modes 1–4.

Mode 1: The probability that the system operates in mode 1 can be computed as

$$\mathbb{P}(\text{mode 1})=\mathbb{P}\left(I_{T_1,T_2}\geq R\right)\mathbb{P}\left(I_{T_2,T_1}\geq R\right)\approx\mathbb{P}\left(\frac{E_{T_1}}{M_1N_0}\|\mathbf{H}_{T_1,T_2}\|_F^2\geq\tau\right)\times\mathbb{P}\left(\frac{E_{T_2}}{M_2N_0}\|\mathbf{H}_{T_2,T_1}\|_F^2\geq\tau\right) \quad (29)$$

where the second step follows from Jensen's approximation and $\tau=(2^{R/\min(M_1,M_2)}-1)\min(M_1,M_2)$. Noting the fact that $\frac{E_{T_1}}{M_1N_0}\|\mathbf{H}_{T_1,T_2}\|_F^2\sim\text{Gamma}(M_1M_2,\overline{\gamma}_{T_1,T_2})$ and $\frac{E_{T_2}}{M_2N_0}\|\mathbf{H}_{T_2,T_1}\|_F^2\sim\text{Gamma}(M_1M_2,\overline{\gamma}_{T_2,T_1})$, where $\overline{\gamma}_{T_1,T_2}=E_{T_1}\sigma_{T_1,T_2}^2/M_1N_0$ and $\overline{\gamma}_{T_2,T_1}=E_{T_2}\sigma_{T_2,T_1}^2/M_2N_0$, (29) can be obtained as

$$\mathbb{P}(\text{mode 1})=\frac{\Gamma\left(M_1M_2\,,\,\frac{\tau}{\overline{\gamma}_{T_1,T_2}}\right)}{\Gamma(M_1M_2)}\times\frac{\Gamma\left(M_1M_2\,,\,\frac{\tau}{\overline{\gamma}_{T_2,T_1}}\right)}{\Gamma(M_1M_2)}. \quad (30)$$

Obviously, in this mode, T_1 and T_2 successfully decode their intended signals by relying on the direct links. Thus, we have

$$P_{\text{out}|\text{mode 1}}^{\text{I-TDBC-CSM}}(R)=0. \quad (31)$$

Mode 2: The probability that the system operates in mode 2 can be computed as

$$\mathbb{P}(\text{mode 2})=\mathbb{P}\left(I_{T_1,T_2}\geq R\right)\mathbb{P}\left(I_{T_2,T_1}<R\right)\approx\frac{\Gamma\left(M_1M_2\,,\,\frac{\tau}{\overline{\gamma}_{T_1,T_2}}\right)}{\Gamma(M_1M_2)}\left(1-\frac{\Gamma\left(M_1M_2\,,\,\frac{\tau}{\overline{\gamma}_{T_2,T_1}}\right)}{\Gamma(M_1M_2)}\right) \quad (32)$$

Obviously, in this mode, T_2 successfully decodes its intended signal by relying on the direct transmission. However, the decoding process at T_1 is not successful unless $I_{\mathcal{C},T_1}$ lies above the desired rate R, where $I_{\mathcal{C},T_1}$ is the achievable rate for the MIMO link from $\mathcal{C}$ to T_1, i.e.

$$I_{\mathcal{C},T_1}=\mu_{\mathcal{C},1}\log_2\det\left(\mathbf{I}_{M_1}+\frac{E}{\theta_{\mathcal{C}}N_0}\mathbf{H}_{\mathcal{C},T_1}\mathbf{H}_{\mathcal{C},T_1}^H\right) \quad (33)$$

where $\mu_{\mathcal{C},1}=\frac{\lceil NM_2/\theta_{\mathcal{C}}\rceil}{N}\approx M_2/\theta_{\mathcal{C}}$. Thus, the outage event corresponding to mode 2 can be described as $\{I_{\mathcal{C},T_1}<R\}$. Following similar steps to (15)–(24), the probability of this event conditioned on $\mathcal{C}$ can be obtained as

$$P_{\text{out}|\text{mode 2},\,\mathcal{C}=\emptyset}^{\text{I-TDBC-CSM}}(R)=1 \quad (34)$$

$$P_{\text{out}|\text{mode 2},\,\mathcal{C}\neq\emptyset}^{\text{I-TDBC-CSM}}(R)=1-\sum_{k=0}^{K}\alpha_{k,1}\frac{\Gamma\left(\theta_{\mathcal{C}}M_1+k\,,\,\phi_{\mathcal{C},1}/\overline{\gamma}_{\min,1}\right)}{\Gamma\left(\theta_{\mathcal{C}}M_1+k\right)} \quad (35)$$

where $\overline{\gamma}_{\min,1}$ and $\alpha_{k,1}$ are given in (19) and (20), respectively, and $\phi_{\mathcal{C},1}=\left(2^{R/\mu_{\mathcal{C},1}\delta_1}-1\right)\delta_1$. Following similar steps to those in Appendix A, the PMF of the set $\mathcal{C}$ can be described as

$$\mathbb{P}\left(\mathcal{C}|\text{mode 2}\right)=\prod_{\ell\in\mathcal{C}}\frac{\Gamma\left(M_2,\frac{2^R-1}{\overline{\gamma}_{T_2,\ell}}\right)}{\Gamma(M_2)}\prod_{j\notin\mathcal{C}}\left(1-\frac{\Gamma\left(M_2,\frac{2^R-1}{\overline{\gamma}_{T_2,j}}\right)}{\Gamma(M_2)}\right) \quad (36)$$

This article has been accepted for publication in a future issue of this journal, but has not been fully edited. Content may change prior to final publication. Citation information: DOI 10.1109/TVT.2018.2867894, IEEE Transactions on Vehicular Technology

Substituting (34)–(36) into

$$P_{\text{out}|\text{mode 2}}^{\text{I-TDBC-CSM}}(R) = \sum_{\mathcal{C}} P_{\text{out}|\text{mode 2},\,\mathcal{C}}^{\text{I-TDBC-CSM}}(R)\,\mathbb{P}(\mathcal{C}|\text{mode 2}) \tag{37}$$

we get

$$\begin{aligned} P_{\text{out}|\text{mode 2}}^{\text{I-TDBC-CSM}}(R) &= \prod_{j\in\mathcal{P}}\left(1-\frac{\Gamma\left(M_2,\frac{2^R-1}{\overline{\gamma}_{T_2,j}}\right)}{\Gamma(M_2)}\right) \\ &+ \sum_{\mathcal{C}\neq\emptyset}\left\{\left(1-\sum_{k=0}^{K}\alpha_{k,1}\frac{\Gamma\left(\theta_{\mathcal{C}}M_1+k\,,\frac{\phi_{\mathcal{C},1}}{\overline{\gamma}_{\min,1}}\right)}{\Gamma\left(\theta_{\mathcal{C}}M_1+k\right)}\right)\right. \\ &\times\left.\prod_{\ell\in\mathcal{C}}\frac{\Gamma\left(M_2,\frac{2^R-1}{\overline{\gamma}_{T_2,\ell}}\right)}{\Gamma(M_2)}\prod_{j\notin\mathcal{C}}\left(1-\frac{\Gamma\left(M_2,\frac{2^R-1}{\overline{\gamma}_{T_2,j}}\right)}{\Gamma(M_2)}\right)\right\}. \end{aligned} \tag{38}$$

Mode 3: In a similar fashion to mode 2, the following results can be obtained:

$$\begin{aligned} \mathbb{P}(\text{mode 3}) &= \left(1-\frac{\Gamma\left(M_1M_2,\frac{\tau}{\overline{\gamma}_{T_1,T_2}}\right)}{\Gamma(M_1M_2)}\right) \\ &\times\frac{\Gamma\left(M_1M_2,\frac{\tau}{\overline{\gamma}_{T_2,T_1}}\right)}{\Gamma(M_1M_2)} \end{aligned} \tag{39}$$

$$\begin{aligned} P_{\text{out}|\text{mode 3}}^{\text{I-TDBC-CSM}}(R) &= \prod_{j\in\mathcal{P}}\left(1-\frac{\Gamma\left(M_1,\frac{2^R-1}{\overline{\gamma}_{T_1,j}}\right)}{\Gamma(M_1)}\right) \\ &+ \sum_{\mathcal{C}\neq\emptyset}\left\{\left(1-\sum_{k=0}^{K}\alpha_{k,2}\frac{\Gamma\left(\theta_{\mathcal{C}}M_2+k\,,\frac{\phi_{\mathcal{C},2}}{\overline{\gamma}_{\min,2}}\right)}{\Gamma\left(\theta_{\mathcal{C}}M_2+k\right)}\right)\right. \\ &\times\left.\prod_{\ell\in\mathcal{C}}\frac{\Gamma\left(M_1,\frac{2^R-1}{\overline{\gamma}_{T_1,\ell}}\right)}{\Gamma(M_1)}\prod_{j\notin\mathcal{C}}\left(1-\frac{\Gamma\left(M_1,\frac{2^R-1}{\overline{\gamma}_{T_1,j}}\right)}{\Gamma(M_1)}\right)\right\} \end{aligned} \tag{40}$$

where $\overline{\gamma}_{\min,2}$ and $\alpha_{k,2}$ are given in (19) and (20), respectively, and $\phi_{\mathcal{C},2} = \left(2^{R/\mu_{\mathcal{C},2}\delta_2}-1\right)\delta_2$, where $\mu_{\mathcal{C},2} = \frac{\lceil NM_1/\theta_{\mathcal{C}}\rceil}{N} \approx M_1/\theta_{\mathcal{C}}$.

Mode 4: The probability that the system operates in mode 4 can be computed as

$$\begin{aligned} \mathbb{P}(\text{mode 4}) &= \mathbb{P}\left(I_{T_1,T_2}<R\right)\mathbb{P}\left(I_{T_2,T_1}<R\right) \\ &\approx \left(1-\frac{\Gamma\left(M_1M_2,\frac{\tau}{\overline{\gamma}_{T_1,T_2}}\right)}{\Gamma(M_1M_2)}\right) \\ &\times\left(1-\frac{\Gamma\left(M_1M_2,\frac{\tau}{\overline{\gamma}_{T_2,T_1}}\right)}{\Gamma(M_1M_2)}\right). \end{aligned} \tag{41}$$

As described in Section II-C, when the system operates in mode 4, the I-TDBC-CSM scheme behaves the same as the TDBC-CSM scheme. Thus, $P_{\text{out}|\text{mode 4}}^{\text{I-TDBC-CSM}}(R)$ can be expressed in terms of $P_{\text{out}}^{\text{TDBC-CSM}}(R)$ as

$$P_{\text{out}|\text{mode 4}}^{\text{I-TDBC-CSM}}(R) = P_{\text{out}}^{\text{TDBC-CSM}}(R) \tag{42}$$

where $P_{\text{out}}^{\text{TDBC-CSM}}(R)$ is given in (27).

Having obtained the mode-specific outage probabilities and the probability of occurrence of each mode, we can now compute $P_{\text{out}}^{\text{I-TDBC-CSM}}(R)$ in closed form by substituting (30)–(32) and (38)–(42) into (28).

C. MABC-CSM Scheme

Since the broadcast phase of the MABC-CSM scheme is the same as that of the TDBC-CSM scheme, the conditional outage probabilities of both schemes for a given set of reliable relay nodes are equal, i.e. we have

$$P_{\text{out}|\,\mathcal{C}}^{\text{MABC-CSM}}(R) = P_{\text{out}|\,\mathcal{C}}^{\text{TDBC-CSM}}(R) \tag{43}$$

where $P_{\text{out}|\,\mathcal{C}}^{\text{TDBC-CSM}}(R)$ is given in (15) and (24) for $\mathcal{C}=\emptyset$ and $\mathcal{C}\neq\emptyset$, respectively. To average $P_{\text{out}|\,\mathcal{C}}^{\text{MABC-CSM}}(R)$ over $\mathcal{C}$, we first need to compute the PMF of the set $\mathcal{C}$. Based on the definition of $\mathcal{C}$ given in (13), this PMF can be described as

$$\mathbb{P}\left(\mathcal{C}\right) \approx \prod_{\ell\in\mathcal{C}}\mathcal{F}\left(\overline{\gamma}_{T_1,\ell},\overline{\gamma}_{T_2,\ell},R\right)\prod_{j\notin\mathcal{C}}\Big(1-\mathcal{F}\left(\overline{\gamma}_{T_1,j},\overline{\gamma}_{T_2,j},R\right)\Big) \tag{44}$$

where

$$\begin{aligned} \mathcal{F}\left(\overline{\gamma}_{T_1,\ell},\overline{\gamma}_{T_2,\ell},R\right) &\triangleq \frac{\Gamma\left(M_1,\frac{2^R-1}{\overline{\gamma}_{T_1,\ell}}\right)}{\Gamma\left(M_1\right)}\times\frac{\Gamma\left(M_2,\frac{2^{2R}-2^R}{\overline{\gamma}_{T_2,\ell}}\right)}{\Gamma\left(M_2\right)} \\ &+\frac{\Gamma\left(M_1,\frac{2^{2R}-2^R}{\overline{\gamma}_{T_1,\ell}}\right)}{\Gamma\left(M_1\right)}\times\frac{\Gamma\left(M_2,\frac{2^R-1}{\overline{\gamma}_{T_2,\ell}}\right)}{\Gamma\left(M_2\right)} \\ &-\frac{\Gamma\left(M_1,\frac{2^{2R}-2^R}{\overline{\gamma}_{T_1,\ell}}\right)}{\Gamma\left(M_1\right)}\times\frac{\Gamma\left(M_2,\frac{2^{2R}-2^R}{\overline{\gamma}_{T_2,\ell}}\right)}{\Gamma\left(M_2\right)}. \end{aligned} \tag{45}$$

The derivation of (44) is given in Appendix B. Substituting (43) and (44) into

$$P_{\text{out}}^{\text{MABC-CSM}}(R) = \sum_{\mathcal{C}} P_{\text{out}|\,\mathcal{C}}^{\text{MABC-CSM}}(R)\,\mathbb{P}\left(\mathcal{C}\right) \tag{46}$$

we obtain the outage probability in closed form as

$$\begin{aligned} P_{\text{out}}^{\text{MABC-CSM}}(R) &= \prod_{j\in\mathcal{P}}\Big(1-\mathcal{F}(\overline{\gamma}_{T_1,j},\overline{\gamma}_{T_2,j},R)\Big) \\ &+\sum_{\mathcal{C}\neq\emptyset}\left\{\left(1-\prod_{i=1}^{2}\sum_{k=0}^{K}\alpha_{k,i}\frac{\Gamma\left(\theta_{\mathcal{C}}M_i+k\,,\frac{\psi_{\mathcal{C},i}}{\overline{\gamma}_{\min,i}}\right)}{\Gamma\left(\theta_{\mathcal{C}}M_i+k\right)}\right)\right. \\ &\times\left.\prod_{\ell\in\mathcal{C}}\mathcal{F}(\overline{\gamma}_{T_1,\ell},\overline{\gamma}_{T_2,\ell},R)\prod_{j\notin\mathcal{C}}\Big(1-\mathcal{F}(\overline{\gamma}_{T_1,j},\overline{\gamma}_{T_2,j},R)\Big)\right\}. \end{aligned} \tag{47}$$

IV. Average Transmission Rate Analysis

As described in Section II, in all of the three CSM-based schemes, the transmission rate varies depending on the number of reliable relay nodes. Moreover, in the I-TDBC-CSM scheme, the transmission rate also depends on the success or failure of the direct transmissions. One of the most important performance measures that characterizes the merits of a variable-rate protocol is the average transmission rate[2] [1], [38]. In this section, we investigate the proposed schemes

[2]This performance measure should not be confused with the ergodic capacity.

This article has been accepted for publication in a future issue of this journal, but has not been fully edited. Content may change prior to final publication. Citation information: DOI 10.1109/TVT.2018.2867894, IEEE Transactions on Vehicular Technology

in terms of this performance measure. We can easily show that the amount of signaling overhead is negligible compared with the number of symbols exchanged between the transceivers. Thus, in the following analysis, we ignore it.

A. TDBC-CSM Scheme

As described in Section II-B, for a given set of reliable relay nodes $\mathcal{C}$, the number of required symbol intervals for the exchange of $N(M_1+M_2)$ information symbols between T_1 and T_2 equals $2N+\lceil N\max(M_1,M_2)/\theta_{\mathcal{C}}\rceil$. Thus, the transmission rate[3] conditioned on the set $\mathcal{C}$ can be expressed as

$$\begin{aligned}\mathcal{R}_{\text{sum}\,|\,\mathcal{C}}^{\text{TDBC-CSM}} &= \frac{N(M_1+M_2)}{2N+\lceil N\max(M_1,M_2)/\theta_{\mathcal{C}}\rceil}\,R \\ &\approx \frac{\theta_{\mathcal{C}}(M_1+M_2)}{2\,\theta_{\mathcal{C}}+\max(M_1,M_2)}\,R. \end{aligned} \tag{48}$$

By averaging $\mathcal{R}_{\text{sum}\,|\,\mathcal{C}}^{\text{TDBC-CSM}}$ over $\mathcal{C}$, the average transmission rate can be obtained in closed form as

$$\begin{aligned}\mathcal{R}_{\text{sum}}^{\text{TDBC-CSM}} &= \sum_{\mathcal{C}} \mathcal{R}_{\text{sum}\,|\,\mathcal{C}}^{\text{TDBC-CSM}}\;\mathbb{P}\left(\mathcal{C}\right) \\ &= \sum_{\mathcal{C}}\Bigg\{\frac{\theta_{\mathcal{C}}(M_1+M_2)}{2\,\theta_{\mathcal{C}}+\max(M_1,M_2)}\,R \\ &\times\prod_{\ell\in\mathcal{C}}\left(\frac{\Gamma\left(M_1,\frac{2^R-1}{\overline{\gamma}_{T_1,\ell}}\right)}{\Gamma(M_1)}\times\frac{\Gamma\left(M_2,\frac{2^R-1}{\overline{\gamma}_{T_2,\ell}}\right)}{\Gamma(M_2)}\right) \\ &\times\prod_{j\notin\mathcal{C}}\left(1-\frac{\Gamma\left(M_1,\frac{2^R-1}{\overline{\gamma}_{T_1,j}}\right)}{\Gamma(M_1)}\times\frac{\Gamma\left(M_2,\frac{2^R-1}{\overline{\gamma}_{T_2,j}}\right)}{\Gamma(M_2)}\right)\Bigg\}\end{aligned} \tag{49}$$

where the second step follows from (26).

By letting $\overline{\gamma}_{T_1,\ell}\to\infty$ and $\overline{\gamma}_{T_2,\ell}\to\infty$ in (49), we can also study the asymptotic behavior of $\mathcal{R}_{\text{sum}}^{\text{TDBC-CSM}}$. The asymptotic average rate, denoted by $\widetilde{\mathcal{R}}_{\text{sum}}^{\text{TDBC-CSM}}$, can be calculated as

$$\begin{aligned}\widetilde{\mathcal{R}}_{\text{sum}}^{\text{TDBC-CSM}} &= \lim_{\substack{\overline{\gamma}_{T_1,j}\to\infty\\ \overline{\gamma}_{T_2,j}\to\infty}} \mathcal{R}_{\text{sum}}^{\text{TDBC-CSM}} \\ &= \frac{L(M_1+M_2)}{2\,L+\max(M_1,M_2)}\,R. \end{aligned} \tag{50}$$

The derivation of (50) is given in Appendix C. For comparison, we look at the asymptotic average rates of the following two basic schemes: (i) the conventional TDBC scheme, and; (ii) the case that two half-duplex transceivers directly exchange information with each other[4]:

$$\widetilde{\mathcal{R}}_{\text{sum}}^{\text{TDBC}} = \frac{M_1+M_2}{2+\max(M_1,M_2)}\,R \tag{51}$$

$$\widetilde{\mathcal{R}}_{\text{sum}}^{\text{HD-direct}} = \frac{M_1+M_2}{2}\,R. \tag{52}$$

[3]We characterize the performance of the system in terms of the sum transmission rate (i.e. 1→2 + 2→1).

[4]In this scheme, it is assumed that the two transceivers are able to communicate with each other directly without the help of the relay nodes, as opposed to our system model in which the help of the relay nodes is needed. Although the assumption of this scheme is not the same as our assumption, this scheme can provide a benchmark for the average transmission rate.

Remark:

1) We observe that as L increases, $\widetilde{\mathcal{R}}_{\text{sum}}^{\text{TDBC-CSM}}$ tends to $\frac{1}{2}(M_1+M_2)R$, i.e. the asymptotic average rate linearly scales with the total number of antennas employed by T_1 and T_2. This implies that the TDBC-CSM scheme asymptotically behaves similar to the case that T_1 and T_2 are able to directly exchange information with each other. This observation reveals that the TDBC-CSM scheme effectively overcomes the half-duplex limitation of the relay nodes.
2) To compare the TDBC-CSM and conventional TDBC schemes, we compute the following ratio:
$$\frac{\widetilde{\mathcal{R}}_{\text{sum}}^{\text{TDBC-CSM}}}{\widetilde{\mathcal{R}}_{\text{sum}}^{\text{TDBC}}} = \frac{L(2+\max(M_1,M_2))}{2L+\max(M_1,M_2)}. \tag{53}$$
Clearly, this ratio is greater than 1 and tends to $1+\frac{1}{2}\max(M_1,M_2)$ as L goes to infinity. This implies that the TDBC-CSM scheme outperforms the conventional TDBC scheme in terms of the average transmission rate. Moreover, the performance gain of the TDBC-CSM scheme over the conventional TDBC scheme enhances with increasing M_1 and/or M_2.
3) It is seen that if one or both of the transceivers are equipped with a massive antenna array, $\widetilde{\mathcal{R}}_{\text{sum}}^{\text{TDBC-CSM}}$ scales linearly with the number of potential relay nodes, as opposed to the conventional TDBC scheme in which the average rate is not scalable with L under the massive antenna array conditions.

B. I-TDBC-CSM Scheme

Let $\mathcal{R}_{\text{sum}\,|\,\text{mode}\,m}^{\text{I-TDBC-CSM}}$ denote the average transmission rate corresponding to the case that the system operates in mode m, where $m=1,...,4$. Using the total probability theorem, the average transmission rate can be calculated as

$$\mathcal{R}_{\text{sum}}^{\text{I-TDBC-CSM}} = \sum_{m=1}^{4}\mathcal{R}_{\text{sum}\,|\,\text{mode}\,m}^{\text{I-TDBC-CSM}}\,\mathbb{P}(\text{mode}\,m) \tag{54}$$

where $\mathbb{P}(\text{mode}\,m)$ is given in (30), (32), (39) and (41) for $m=1,\ldots,4$, respectively. Thus, to obtain $\mathcal{R}_{\text{sum}}^{\text{I-TDBC-CSM}}$, we only need to compute the mode-specific rates corresponding to modes 1–4.

Mode 1: In this mode of operation, the exchange of $N(M_1+M_2)$ information symbols between T_1 and T_2 is completed within $2N$ symbol intervals. Thus, we can write

$$\mathcal{R}_{\text{sum}\,|\,\text{mode}\,1}^{\text{I-TDBC-CSM}} = \frac{M_1+M_2}{2}\,R. \tag{55}$$

Mode 2: When the system operates in mode 2, the transmission rate depends on the cardinality of the set $\mathcal{C}$. For a given $\mathcal{C}$, the exchange of $N(M_1+M_2)$ information symbols between T_1 and T_2 requires $2N+\lceil NM_2/\theta_{\mathcal{C}}\rceil$ symbol intervals. Thus, the conditional transmission rate can be written as

$$\begin{aligned}\mathcal{R}_{\text{sum}|\,\text{mode}\,2,\,\mathcal{C}}^{\text{I-TDBC-CSM}} &= \frac{N(M_1+M_2)}{2N+\lceil NM_2/\theta_{\mathcal{C}}\rceil}\,R \\ &\approx \frac{\theta_{\mathcal{C}}(M_1+M_2)}{2\,\theta_{\mathcal{C}}+M_2}\,R. \end{aligned} \tag{56}$$

This article has been accepted for publication in a future issue of this journal, but has not been fully edited. Content may change prior to final publication. Citation information: DOI 10.1109/TVT.2018.2867894, IEEE Transactions on Vehicular Technology

Averaging (56) over $\mathcal{C}$, we obtain

$$\mathcal{R}_{\text{sum}|\text{ mode 2}}^{\text{I-TDBC-CSM}} = \sum_{\mathcal{C}} \mathcal{R}_{\text{sum}|\text{ mode 2},\mathcal{C}}^{\text{I-TDBC-CSM}} \ \mathbb{P}\left(\mathcal{C} \,|\, \text{mode 2}\right)$$
$$= \sum_{\mathcal{C}} \left\{ \frac{\theta_{\mathcal{C}}(M_1+M_2)}{2\,\theta_{\mathcal{C}}+M_2} R \prod_{\ell\in\mathcal{C}} \frac{\Gamma\left(M_2, \frac{2^R-1}{\overline{\gamma}_{T_2,\ell}}\right)}{\Gamma(M_2)} \times \prod_{j\notin\mathcal{C}} \left(1 - \frac{\Gamma\left(M_2, \frac{2^R-1}{\overline{\gamma}_{T_2,j}}\right)}{\Gamma(M_2)}\right)\right\}. \quad (57)$$

Mode 3: By replacing M_1 and M_2 with each other and substituting $\overline{\gamma}_{T_2,j}$ with $\overline{\gamma}_{T_1,j}$ in (57), the transmission rate corresponding to mode 3 can be written as

$$\mathcal{R}_{\text{sum}|\text{ mode 3}}^{\text{I-TDBC-CSM}} = \sum_{\mathcal{C}} \left\{ \frac{\theta_{\mathcal{C}}(M_1+M_2)}{2\,\theta_{\mathcal{C}}+M_1} R \prod_{\ell\in\mathcal{C}} \frac{\Gamma\left(M_1, \frac{2^R-1}{\overline{\gamma}_{T_1,\ell}}\right)}{\Gamma(M_1)} \times \prod_{j\notin\mathcal{C}} \left(1 - \frac{\Gamma\left(M_1, \frac{2^R-1}{\overline{\gamma}_{T_1,j}}\right)}{\Gamma(M_1)}\right)\right\}. \quad (58)$$

Mode 4: Noting the fact that in mode 4, the TDBC-CSM scheme and its incremental counterpart are equivalent, we can write

$$\mathcal{R}_{\text{sum}|\text{ mode 4}}^{\text{I-TDBC-CSM}} = \mathcal{R}_{\text{sum}}^{\text{TDBC-CSM}} \quad (59)$$

where $\mathcal{R}_{\text{sum}}^{\text{TDBC-CSM}}$ is given in (49).

Having obtained the mode-specific transmission rates, the average transmission rate can now be expressed in closed form by substituting (55) and (57)–(59) into (54).

By letting $\overline{\gamma}_{T_1,T_2} \to \infty$ and $\overline{\gamma}_{T_2,T_1} \to \infty$ in (30), (32), (39) and (41), and noting the fact that $\lim_{t_2\to 0} \Gamma(t_1,t_2) = \Gamma(t_1)$, we obtain

$$\lim_{\substack{\overline{\gamma}_{T_1,T_2}\to\infty \\ \overline{\gamma}_{T_2,T_1}\to\infty}} \mathbb{P}(\text{mode } m) = \begin{cases} 1, & m=1 \\ 0, & m=2,3,4. \end{cases} \quad (60)$$

Thus, the asymptotic average rate can be computed as

$$\widetilde{\mathcal{R}}_{\text{sum}}^{\text{I-TDBC-CSM}} = \lim_{\substack{\overline{\gamma}_{T_1,T_2}\to\infty \\ \overline{\gamma}_{T_2,T_1}\to\infty}} \mathcal{R}_{\text{sum}}^{\text{I-TDBC-CSM}} = \frac{M_1+M_2}{2} R. \quad (61)$$

Remark:

1) By comparing (61) and (52), it is seen that the asymptotic average rate of the I-TDBC-CSM scheme equals that of the direct transmission scheme irrespective of the number of potential relay nodes, as opposed to the TDBC-CSM scheme where the asymptotic average rate depends on L. This observation reveals that the I-TDBC-CSM scheme effectively overcomes the rate loss incurred due to the half-duplex limitation of the relay nodes even when L is not large.
2) To compare the TDBC-CSM and I-TDBC-CSM schemes, we compute the ratio

$$\frac{\widetilde{\mathcal{R}}_{\text{sum}}^{\text{I-TDBC-CSM}}}{\widetilde{\mathcal{R}}_{\text{sum}}^{\text{TDBC-CSM}}} = \frac{2L+\max(M_1,M_2)}{2L} \quad (62)$$

which is greater than 1. We therefore conclude that the I-TDBC-CSM scheme outperforms the TDBC-CSM scheme in terms of the average transmission rate. It is also seen that as L increases, the performance of the TDBC-CSM scheme tends to that of the I-TDBC-CSM scheme.

C. MABC-CSM Scheme

Noting the fact that the exchange of $N(M_1+M_2)$ information symbols between T_1 and T_2 is completed within $N+\lceil N\max(M_1,M_2)/\theta_{\mathcal{C}}\rceil$ symbol intervals, the transmission rate conditioned on the set $\mathcal{C}$ can be written as

$$\mathcal{R}_{\text{sum}\,|\,\mathcal{C}}^{\text{MABC-CSM}} = \frac{N(M_1+M_2)}{N+\lceil N\max(M_1,M_2)/\theta_{\mathcal{C}}\rceil} R \approx \frac{\theta_{\mathcal{C}}(M_1+M_2)}{\theta_{\mathcal{C}}+\max(M_1,M_2)} R. \quad (63)$$

Averaging (63) over $\mathcal{C}$, the average transmission rate can be calculated in closed form as

$$\mathcal{R}_{\text{sum}}^{\text{MABC-CSM}} = \sum_{\mathcal{C}} \mathcal{R}_{\text{sum}\,|\,\mathcal{C}}^{\text{MABC-CSM}} \ \mathbb{P}\left(\mathcal{C}\right) = \sum_{\mathcal{C}} \left\{ \frac{\theta_{\mathcal{C}}(M_1+M_2)}{\theta_{\mathcal{C}}+\max(M_1,M_2)} R \times \prod_{\ell\in\mathcal{C}} \mathcal{F}(\overline{\gamma}_{T_1,\ell},\overline{\gamma}_{T_2,\ell},R) \times \prod_{j\notin\mathcal{C}} \left[1-\mathcal{F}(\overline{\gamma}_{T_1,j},\overline{\gamma}_{T_2,j},R)\right]\right\} \quad (64)$$

where the second step follows from (44).

By letting $\overline{\gamma}_{T_1,\ell}$ and $\overline{\gamma}_{T_2,\ell}$ in (64) go to infinity, the asymptotic average rate can be obtained as

$$\widetilde{\mathcal{R}}_{\text{sum}}^{\text{MABC-CSM}} = \frac{L(M_1+M_2)}{L+\max(M_1,M_2)} R \quad (65)$$

where to obtain (65), we have used the fact that $\lim_{\overline{\gamma}_{T_1,\ell},\overline{\gamma}_{T_2,\ell}\to\infty} \mathcal{F}(\overline{\gamma}_{T_1,\ell},\overline{\gamma}_{T_2,\ell},R) = 1$.

For comparison, we consider the following two basic schemes: (i) the conventional MABC scheme, and; (ii) the case that two full-duplex transceivers directly exchange information:

$$\widetilde{\mathcal{R}}_{\text{sum}}^{\text{MABC}} = \frac{M_1+M_2}{1+\max(M_1,M_2)} R \quad (66)$$

$$\widetilde{\mathcal{R}}_{\text{sum}}^{\text{FD-direct}} = (M_1+M_2)\,R. \quad (67)$$

Remark:

1) It is worth noting that with increasing the number of potential relay nodes, $\widetilde{\mathcal{R}}_{\text{sum}}^{\text{MABC-CSM}}$ tends to $\widetilde{\mathcal{R}}_{\text{sum}}^{\text{FD-direct}}$. This observation reveals that the MABC-CSM scheme asymptotically behaves similar to the case that two full-duplex transceivers directly exchange information with each other. This implies that the MABC-CSM scheme not only overcomes the half-duplex limitation of the relay nodes but also mitigates the spectral efficiency loss incurred due to the half-duplex limitation of the transceivers.

This article has been accepted for publication in a future issue of this journal, but has not been fully edited. Content may change prior to final publication. Citation information: DOI 10.1109/TVT.2018.2867894, IEEE Transactions on Vehicular Technology

$$\Delta^{\text{TDBC-CSM}}(r) = \min(M_1, M_2) \min_{0\le\theta_{\mathcal{C}}\le L} \left\{ \left(1 - \frac{2\,L + M_{j_0}}{L(M_1+M_2)}\, r\right)^{+} (L-\theta_{\mathcal{C}}) + \left(1 - \frac{2\,L + M_{j_0}}{L(M_1+M_2)\mu_{\mathcal{C}}\delta_{i_0}}\, r\right)^{+} \theta_{\mathcal{C}} \right\} \quad (74)$$

$$\begin{aligned}\Delta^{\text{I-TDBC-CSM}}(r) = \min_{0\le\theta_{\mathcal{C}}\le L} \Bigg\{ & \left(1 - \frac{2\,r}{(M_1+M_2)M_{i_0}}\right)^{+} M_1M_2 + \left(1 - \frac{2\,r}{M_1+M_2}\right)^{+} (L-\theta_{\mathcal{C}})M_2 + \left(1 - \frac{2\,r}{(M_1+M_2)\mu_{\mathcal{C},1}\delta_1}\right)^{+} \theta_{\mathcal{C}} M_1, \\ & \left(1 - \frac{2\,r}{(M_1+M_2)M_{i_0}}\right)^{+} M_1M_2 + \left(1 - \frac{2\,r}{M_1+M_2}\right)^{+} (L-\theta_{\mathcal{C}})M_1 + \left(1 - \frac{2\,r}{(M_1+M_2)\mu_{\mathcal{C},2}\delta_2}\right)^{+} \theta_{\mathcal{C}} M_2, \\ & 2\left(1 - \frac{2\,r}{(M_1+M_2)M_{i_0}}\right)^{+} M_1M_2 + \left(1 - \frac{2\,r}{M_1+M_2}\right)^{+} (L-\theta_{\mathcal{C}})M_{i_0} + \left(1 - \frac{2\,r}{(M_1+M_2)\mu_{\mathcal{C}}\delta_{i_0}}\right)^{+} \theta_{\mathcal{C}} M_{i_0} \Bigg\}\end{aligned} \quad (75)$$

$$\begin{aligned}\Delta^{\text{MABC-CSM}}(r) = \min_{0\le\theta_{\mathcal{C}}\le L} \Bigg\{ & \left(1 - \frac{L + M_{j_0}}{L(M_1+M_2)}\, r\right)^{+} (L-\theta_{\mathcal{C}}) \min(M_1, M_2) + \left(1 - \frac{L + M_{j_0}}{L(M_1+M_2)\mu_{\mathcal{C}}\delta_{i_0}}\, r\right)^{+} \theta_{\mathcal{C}} \min(M_1, M_2), \\ & \left(1 - \frac{2(L + M_{j_0})}{L(M_1+M_2)}\, r\right)^{+} (L-\theta_{\mathcal{C}})(M_1+M_2) + \left(1 - \frac{L + M_{j_0}}{L(M_1+M_2)\mu_{\mathcal{C}}\delta_{i_0}}\, r\right)^{+} \theta_{\mathcal{C}} \min(M_1, M_2) \Bigg\}\end{aligned} \quad (76)$$

2) We note that

$$\frac{\widetilde{\mathcal{R}}_{\text{sum}}^{\text{MABC-CSM}}}{\widetilde{\mathcal{R}}_{\text{sum}}^{\text{MABC}}} = \frac{L(1+\max(M_1, M_2))}{L+\max(M_1, M_2)}. \quad (68)$$

This ratio is greater than 1 and tends to $1 + \max(M_1, M_2)$ as L goes to infinity. This observation shows that the MABC-CSM scheme outperforms the conventional MABC scheme in terms of the average transmission rate. Moreover, the performance gain of the MABC-CSM scheme over the conventional MABC scheme enhances with increasing M_1 and/or M_2.

3) We observe that if one of the transceivers is equipped with a massive antenna array, $\widetilde{\mathcal{R}}_{\text{sum}}^{\text{MABC-CSM}}$ increases up to LR. In the conventional MABC scheme, this quantity equals R. If both of the transceivers are equipped with massive antenna arrays, $\widetilde{\mathcal{R}}_{\text{sum}}^{\text{MABC-CSM}}$ tends to $2LR$, which is L times $\widetilde{\mathcal{R}}_{\text{sum}}^{\text{MABC}}$.

V. DMT Analysis

In this section, we analyze the proposed schemes in terms of the DMT, i.e. the diversity order as a function of the multiplexing gain [39], [40].

Lemma 1: The upper incomplete gamma function can be expressed asymptotically as

$$\Gamma(t_1, t_2) \sim \Gamma(t_1) - (t_2)^{t_1}/t_1 \quad \text{as} \quad t_2 \to 0. \quad (69)$$

Proof: See Appendix D. ∎

Proposition 1: The TDBC-CSM scheme achieves the DMT of (74), shown at the top of the page, where $\Delta(.)$ is the diversity order, r is the multiplexing gain, $i_0 = \arg\min_{1\le i\le 2} M_i$ and $j_0 = \arg\max_{1\le i\le 2} M_i$.

Proof: Without loss of generality and for ease of exposition, let $E_{T_1}/N_0 = \epsilon_1\mathsf{SNR}$, $E_{T_2}/N_0 = \epsilon_2\mathsf{SNR}$ and $E/N_0 = \epsilon_3\mathsf{SNR}$, where SNR is a reference signal-to-noise ratio and ϵ_1, ϵ_2 and ϵ_3 are three positive constants indicating the power ratios allocated to T_1, T_2 and the set of reliable relay nodes, respectively. Thus, $\overline{\gamma}_{T_1,\ell}$, $\overline{\gamma}_{T_2,\ell}$ and $\overline{\gamma}_{\ell_j,T_i}$ can be written as a function of SNR as $\overline{\gamma}_{T_1,\ell} = \xi_{T_1,\ell}\mathsf{SNR}$, $\overline{\gamma}_{T_2,\ell} = \xi_{T_2,\ell}\mathsf{SNR}$, and $\overline{\gamma}_{\ell_j,T_i} = \xi_{\ell_j,T_i}\mathsf{SNR}$, where $\xi_{T_1,\ell} = \epsilon_1\sigma_{T_1,\ell}^2/M_1$, $\xi_{T_2,\ell} = \epsilon_2\sigma_{T_2,\ell}^2/M_2$, and $\xi_{\ell_j,T_i} = \epsilon_3\sigma_{\ell_j,T_i}^2/\theta_{\mathcal{C}}$. For a variable-rate protocol, the multiplexing gain is defined as the ratio of the average transmission rate to $\log\mathsf{SNR}$ as SNR goes to infinity [38]. Thus, $\mathcal{R}_{\text{sum}}^{\text{TDBC-CSM}}$ can be described as

$$\mathcal{R}_{\text{sum}}^{\text{TDBC-CSM}} \sim r\log\mathsf{SNR}. \quad (70)$$

Substituting (70) into (50), we obtain $R \sim \eta\, r\log\mathsf{SNR}$, where $\eta = [2\,L + \max(M_1, M_2)]/L(M_1+M_2)$. Having obtained the asymptotic behavior of R, the diversity order as a function of the multiplexing gain can now be formulated as

$$\Delta^{\text{TDBC-CSM}}(r) = -\lim_{\mathsf{SNR}\to\infty} \frac{\log P_{\text{out}}^{\text{TDBC-CSM}}(\eta\, r\log\mathsf{SNR})}{\log\mathsf{SNR}} \quad (71)$$

Let us focus on the numerator of (71). Based on Lemma 1, for $r < \eta^{-1}$, we can write the following asymptotic expression:

$$\Gamma\left(M_i, \frac{2^R-1}{\overline{\gamma}_{T_i,\ell}}\right) \sim \Gamma(M_i) - \frac{1}{M_i}\left(\frac{\mathsf{SNR}^{\eta r-1}}{\xi_{T_i,\ell}}\right)^{M_i} \quad (72)$$

where $i = 1, 2$. For $r > \eta^{-1}$, the left-hand side of (72) tends to zero as SNR goes to infinity. Similarly, for $r < \eta^{-1}\mu_{\mathcal{C}}\delta_i$, we have

$$\begin{aligned}\Gamma\left(\theta_{\mathcal{C}}M_i + k\,, \frac{\psi_{\mathcal{C},i}}{\overline{\gamma}_{\min,i}}\right) \sim{}& \Gamma(\theta_{\mathcal{C}}M_i + k) - (\theta_{\mathcal{C}}M_i + k)^{-1} \\ & \times \left(\frac{\delta_i\mathsf{SNR}^{\frac{\eta r}{\mu_{\mathcal{C}}\delta_i}-1}}{\min\limits_{1\le j\le\theta_{\mathcal{C}}} \xi_{\ell_j,T_i}}\right)^{\theta_{\mathcal{C}}M_i+k}\end{aligned} \quad (73)$$

where $i = 1, 2$. For $r > \eta^{-1}\mu_{\mathcal{C}}\delta_i$, the left-hand side of (73) tends to zero as SNR goes to infinity. Substituting (72) and (73) into (27) and then computing (71), we get (74). ∎

Proposition 2: The I-TDBC-CSM and MABC-CSM schemes achieve the DMTs of (75) and (76), respectively, shown at the top of the page.

This article has been accepted for publication in a future issue of this journal, but has not been fully edited. Content may change prior to final publication. Citation information: DOI 10.1109/TVT.2018.2867894, IEEE Transactions on Vehicular Technology

Proof: Following similar steps to those used for deriving (74), the DMT expressions for the I-TDBC-CSM and MABC-CSM schemes can be obtained as (75) and (76), respectively. We omit the details due to the space limitations. ■

Remark:

1) Based on (74)–(76), we conclude that for a fixed R (i.e. $r = 0$ [39]), the outage probabilities behave asymptotically as

$$P_{\text{out}}^{\text{TDBC-CSM}}(R) \propto \mathsf{SNR}^{-L\min(M_1,M_2)} \tag{77}$$

$$P_{\text{out}}^{\text{I-TDBC-CSM}}(R) \propto \mathsf{SNR}^{-(L\min(M_1,M_2)+M_1M_2)} \tag{78}$$

$$P_{\text{out}}^{\text{MABC-CSM}}(R) \propto \mathsf{SNR}^{-L\min(M_1,M_2)}. \tag{79}$$

These expressions show how fast the rate of unsuccessful information exchange between T_1 and T_2 decays with increasing SNR.

2) Noting the fact that in the absence of the direct link, the number of independent bidirectional paths between T_1 and T_2 is at most $L\min(M_1, M_2)$, we conclude that the TDBC-CSM and MABC-CSM schemes guarantee the maximum achievable diversity gain.
3) Noting the fact that in the presence of the direct link, the number of independent bidirectional paths between T_1 and T_2 is at most $L\min(M_1, M_2) + M_1M_2$, we conclude that the I-TDBC-CSM scheme achieves the full diversity gain.

VI. Simulation Results and Numerical Examples

Throughout our numerical examples, it is assumed that $v = 4$ and $K = 20$. Unless otherwise stated, the curves are plotted under the assumption of equal power allocation, i.e. $\epsilon_1 = \epsilon_2 = \epsilon_3 = 1/3$. Figs. 2–4 show the outage probability of the TDBC-CSM, I-TDBC-CSM and MABC-CSM schemes as a function of SNR for different values of M_1, M_2 and L. From the figures, we observe that the simulation results confirm the theoretical analysis of the paper. We also observe that the slope of the outage probability curves increases with increasing M_1, M_2 and L in the high-SNR regime. This observation confirms the fact that a higher diversity gain is achieved with increasing either of these parameters. From Figs. 2 and 4, we observe that the outage probability curves corresponding to the case $\{M_1 = M_2 = 1,\ L = 2\}$ and the case $\{M_1 = M_2 = 2,\ L = 1\}$ decay with the same slope with increasing SNR in the high-SNR regime. This observation is in agreement with the asymptotic analysis of Section V.

Fig. 5 compares the proposed schemes in terms of the outage probability for different values of R. As we observe, there is no significant gap between the outage probabilities of the TDBC-CSM and I-TDBC-CSM schemes in the low-SNR regime. This is due to the fact that at low SNRs, the direct transmissions usually fail, and hence, the I-TDBC-CSM scheme operates in mode 4 most of the time. Recall that when the system operates in mode 4, there is no difference between the TDBC-CSM and I-TDBC-CSM schemes. We also observe that there is no significant gap between the outage probabilities of the TDBC-CSM and MABC-CSM schemes for small value of the target rate. This can be explained as follows. (i) For small values of R, with high probability, the condition ${}_3I_\ell \geq 2R$ is satisfied in (13). Under these circumstances, (13) reduces to (3). This implies that both of the schemes rely on the same set of relay nodes (intuitively, in the low-R regime, with high probability, the decoding process at the relay node is successful regardless of whether the multiple-access channel is interference-limited or not. Thus, in this case, there is no significant difference between the TDBC-CSM and MABC-CSM schemes in terms of the set of reliable relay nodes). (ii) Recall that for a given set of reliable relay nodes, the TDBC-CSM and MABC-CSM schemes behave the same in terms of the outage probability. These two facts justify what we observe in Fig. 5. On the other hand, we also observe that as the target rate increases, a significant performance gap between these two schemes appears. This is due to the fact that

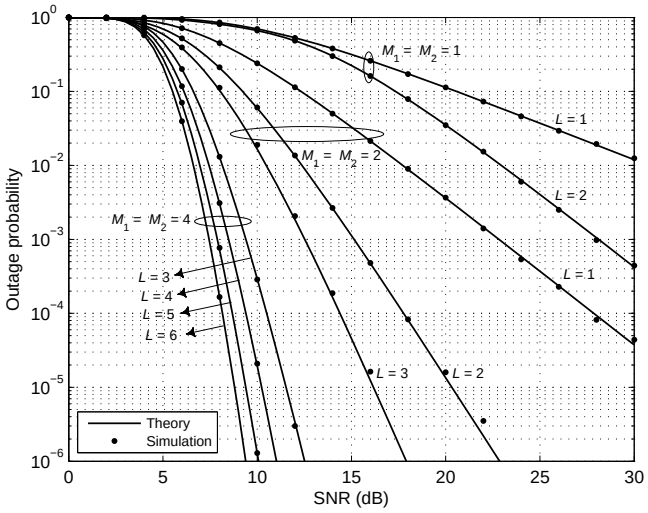

Fig. 2. Outage probability versus SNR for the TDBC-CSM scheme. $R = 1$ bps/Hz and $d_{T_1,\ell} = d_{T_2,\ell} = 0.5\, d_{T_1,T_2}$, for $\ell = 1, ..., L$.

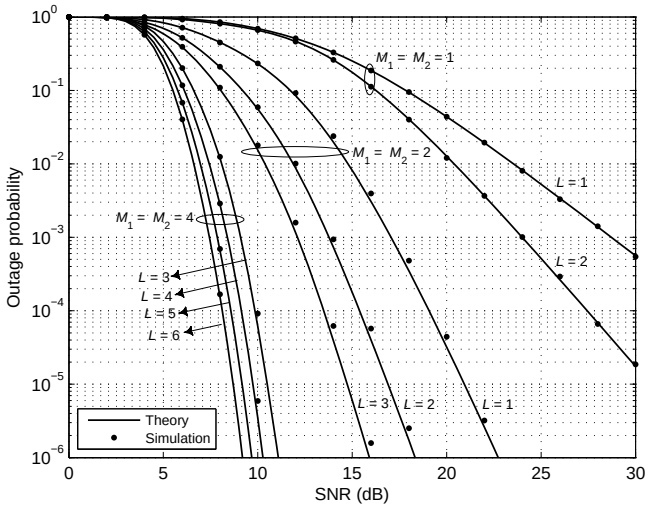

Fig. 3. Outage probability versus SNR for the I-TDBC-CSM scheme. $R = 1$ bps/Hz and $d_{T_1,\ell} = d_{T_2,\ell} = 0.5\, d_{T_1,T_2}$, for $\ell = 1, ..., L$.

This article has been accepted for publication in a future issue of this journal, but has not been fully edited. Content may change prior to final publication. Citation information: DOI 10.1109/TVT.2018.2867894, IEEE Transactions on Vehicular Technology

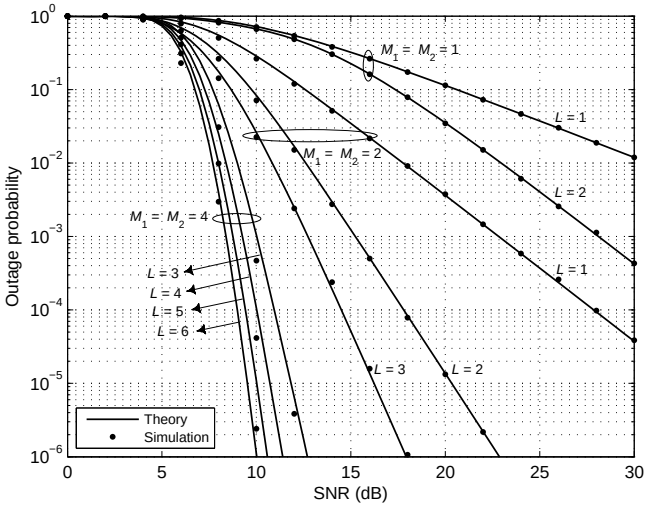

Fig. 4. Outage probability versus SNR for the MABC-CSM scheme. $R = 1$ bps/Hz and $d_{T_1,\ell} = d_{T_2,\ell} = 0.5\, d_{T_1,T_2}$, for $\ell = 1, ..., L$.

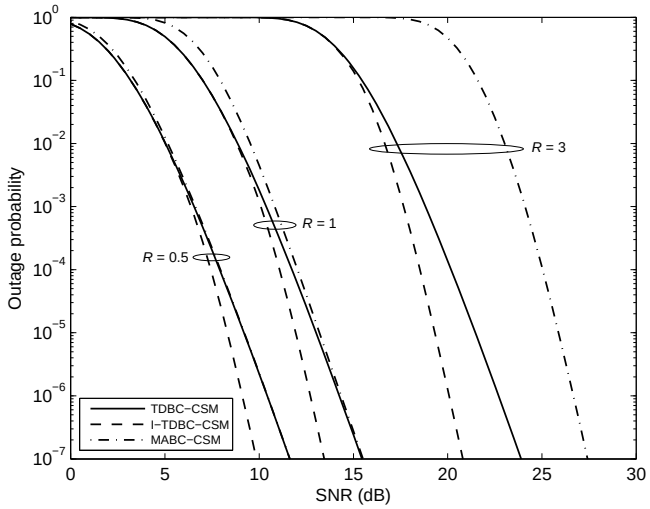

Fig. 5. Outage probability versus SNR. Comparison of different schemes. $M_1 = M_2 = 3$, $L = 3$ and $d_{T_1,\ell} = d_{T_2,\ell} = 0.5\, d_{T_1,T_2}$, for $\ell = 1, ..., L$.

as R increases, it is likely that in (13), the condition ${}_3I_\ell \geq 2R$ cannot be satisfied. Thus, the cardinality of the set of reliable relay nodes in the MABC-CSM scheme is smaller than that in the TDBC-CSM scheme. Thus, we expect the TDBC-CSM scheme to outperform the MABC-CSM scheme (intuitively, since the multiple-access phase of the MABC-CSM scheme is interference-limited, it is likely that the target rate cannot be achieved in the high-R regime, and this increases the risk of outage in the MABC-CSM scheme).

Fig. 6 shows the outage probability as a function of the target rate for different values of SNR. As we observe, the TDBC-CSM and MABC-CSM curves are very close in the low-rate regime, which is in agreement with our observations in Fig. 5. We also observe that in the high-rate regime, the outage probability of the I-TDBC-CSM scheme tends to that of the TDBC-CSM scheme. This is due to the fact that in the high-rate regime, the direct links are not able to support the desired rate and hence, the I-TDBC-CSM scheme switches to the TDBC-CSM scheme. Table I summarizes these observations.

Figs. 7–9 show the average transmission rate of the proposed schemes as a function of SNR for different values of M_1, M_2 and L. As we observe, the simulation results are in good agreement with the theoretical analysis of the paper. Table II compares the proposed schemes in terms of the average transmission rate for different values of R and SNR.

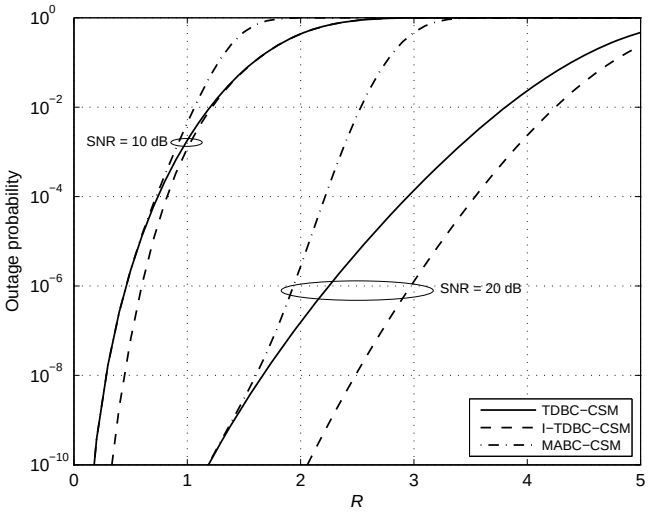

Fig. 6. Outage probability versus R. Comparison of different schemes. $M_1 = M_2 = 3$, $L = 3$ and $d_{T_1,\ell} = d_{T_2,\ell} = 0.5\, d_{T_1,T_2}$, for $\ell = 1, ..., L$.

It is important to note that in Table II, different schemes are compared independent of their outage probability performances. To compare the proposed schemes fairly, we

TABLE I
COMPARISON OF DIFFERENT SCHEMES IN TERMS OF THE OUTAGE PROBABILITY

The symbols $\approx$, $>$ and $\gg$ stand for "almost performs the same as", "performs better than", and "performs much better than", respectively.

R	SNR	Performance comparison
Low	Low	I-TDBC-CSM $\approx$ TDBC-CSM $\approx$ MABC-CSM
Low	High	I-TDBC-CSM $>$ TDBC-CSM $\approx$ MABC-CSM
High	Low	I-TDBC-CSM $\approx$ TDBC-CSM $\gg$ MABC-CSM
High	High	I-TDBC-CSM $\gg$ TDBC-CSM $\gg$ MABC-CSM

TABLE II
COMPARISON OF DIFFERENT SCHEMES IN TERMS OF THE AVERAGE TRANSMISSION RATE

R	SNR	Performance comparison
Low	Low	MABC-CSM $>$ I-TDBC-CSM $\approx$ TDBC-CSM
Low	High	MABC-CSM $>$ I-TDBC-CSM $>$ TDBC-CSM
High	Low	I-TDBC-CSM $\approx$ TDBC-CSM $>$ MABC-CSM
High	High	MABC-CSM $>$ I-TDBC-CSM $>$ TDBC-CSM

This article has been accepted for publication in a future issue of this journal, but has not been fully edited. Content may change prior to final publication. Citation information: DOI 10.1109/TVT.2018.2867894, IEEE Transactions on Vehicular Technology

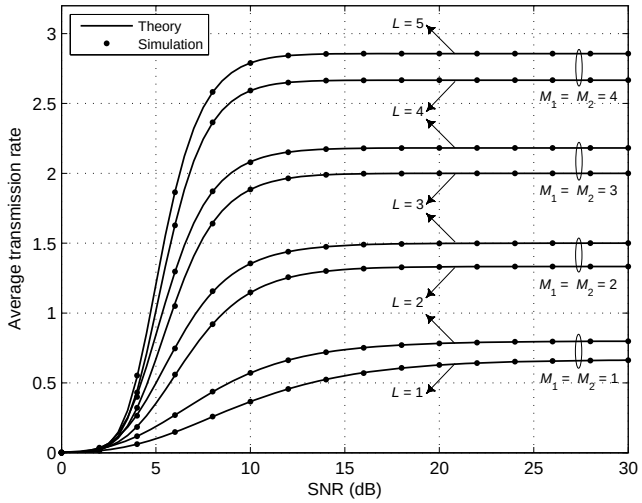

Fig. 7. Average transmission rate versus SNR for the TDBC-CSM scheme. $R = 1$ bps/Hz and $d_{T_1,\ell} = d_{T_2,\ell} = 0.5\, d_{T_1,T_2}$, for $\ell = 1, ..., L$.

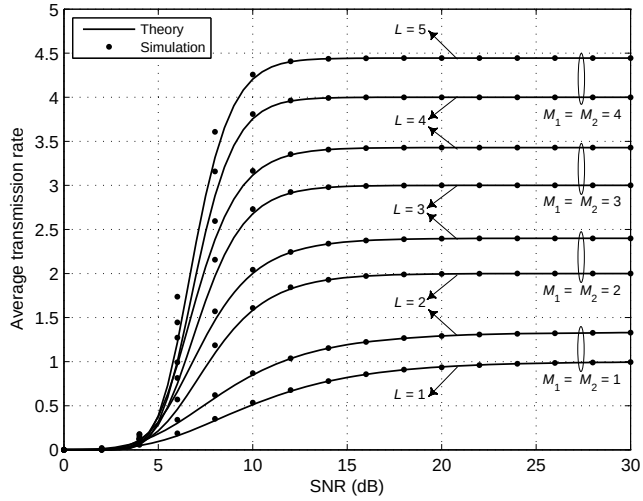

Fig. 9. Average transmission rate versus SNR for the MABC-CSM scheme. $R = 1$ bps/Hz and $d_{T_1,\ell} = d_{T_2,\ell} = 0.5\, d_{T_1,T_2}$, for $\ell = 1, ..., L$.

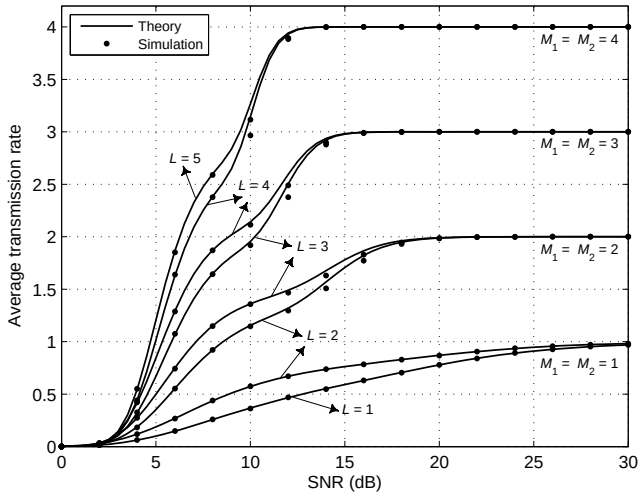

Fig. 8. Average transmission rate versus SNR for the I-TDBC-CSM scheme. $R = 1$ bps/Hz and $d_{T_1,\ell} = d_{T_2,\ell} = 0.5\, d_{T_1,T_2}$, for $\ell = 1, ..., L$.

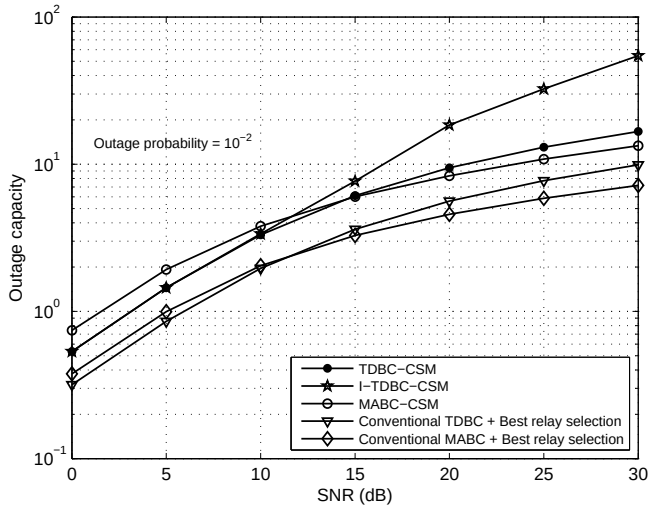

Fig. 10. Outage capacity versus SNR. The outage probability is fixed at 10^{-2}, $M_1 = M_2 = L = 4$, $d_{T_1,\ell} = d_{T_2,\ell} = 0.5\, d_{T_1,T_2}$, for $\ell = 1, ..., L$.

should consider Tables I and II simultaneously. To this end, in Fig. 10, we compare the proposed schemes in terms of the outage capacity (i.e. the maximum transmission rate such that the outage probability does not exceed a target level). In this figure, we fix the outage probability at 10^{-2}. As we observe from the figure, in the high-SNR regime, the I-TDBC-CSM scheme significantly outperforms the other two schemes. The superior performance of this scheme is due to the existence of the direct link and the incremental nature of the protocol that shows itself in the high-SNR regime. It is also interesting to note that in the high-SNR regime, the TDBC-CSM scheme performs slightly better than the MABC-CSM scheme, whereas in the low-SNR regime, the MABC-CSM scheme outperforms the other schemes. To explain this observation, it is sufficient to note that in this figure, the low-SNR and high-SNR regimes are equivalent to the low-R and high-R regimes, respectively. As explained earlier, in the high-R regime, the TDBC-CSM scheme significantly outperforms the MABC-CSM scheme in terms of the outage probability. Thus, for a given outage probability, it is expected that the TDBC-CSM scheme achieves higher transmission rate than the MABC-CSM scheme. On the other hand, in the low-R regime, as explained earlier, there is no significant difference between the outage probabilities of these two schemes. However, due to the nonorthogonality of the multiple-access phase of the MABC-CSM scheme, this scheme achieves higher transmission rate than the TDBC-CSM scheme in which the multiple-access phase is orthogonal. For comparison, in this figure, we have also depicted the outage capacity curves corresponding to the conventional TDBC and MABC schemes. In these two schemes, only the best relay node transmits in the broadcast phase. The best relay node is selected among the reliable relay

This article has been accepted for publication in a future issue of this journal, but has not been fully edited. Content may change prior to final publication. Citation information: DOI 10.1109/TVT.2018.2867894, IEEE Transactions on Vehicular Technology

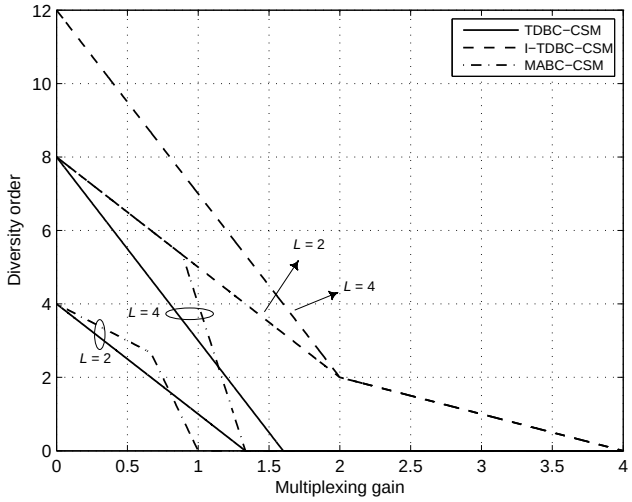

Fig. 11. Diversity-multiplexing tradeoff. $M_1 = M_2 = 2$.

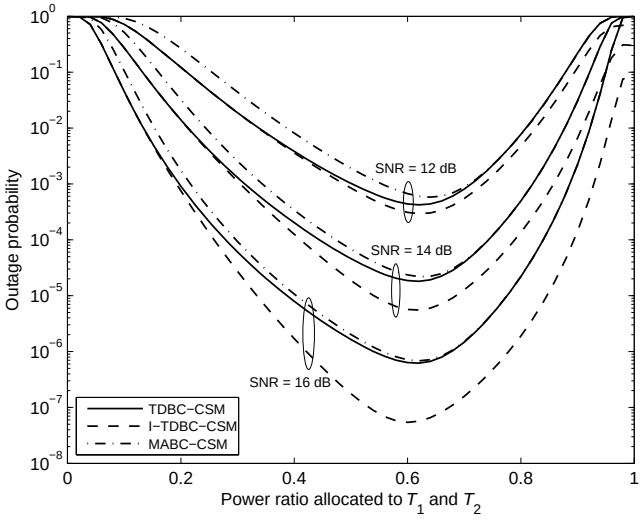

Fig. 12. Outage probability as a function of the power ratio allocated to T_1 and T_2. $M_1 = M_2 = 2$, $L = 4$ and $d_{T_1,\ell} = d_{T_2,\ell} = 0.5\, d_{T_1,T_2}$, for $\ell = 1, ..., L$.

nodes such that the minimum SNR of the relay-T_1 and relay-T_2 links is maximized. We clearly observe that the CSM-based schemes outperform their non-CSM-based counterparts.

Fig. 11 shows the diversity order as a function of the multiplexing gain for different values of L. We clearly observe that with increasing L, a greater diversity order is achieved. Fig. 12 shows the outage probability as a function of the total power ratio allocated to T_1 and T_2, i.e. $\epsilon_1 + \epsilon_2$. It is assumed that $\epsilon_1 = \epsilon_2$ and $\epsilon_1 + \epsilon_2 + \epsilon_3 = 1$. We observe that under these circumstances, allocating equal power to the transceivers and the set of reliable relay nodes is almost optimal in the sense of minimizing the outage probability.

VII. Conclusion

In this paper, we have proposed and analyzed three network-coded CSM schemes for a TWRC with DF relaying. The analysis of the paper showed that the proposed schemes achieve high spectral efficiency and at the same time guarantee the maximum achievable diversity gain. Interestingly, we observed that both of these performance measures improve with increasing the number of potential relay nodes. We, therefore, conclude that the CSM schemes are suitable candidates to meet the growing demand for reliable high data rate communications. In this paper, the relay nodes operate in the DF processing mode. An interesting issue for future work is to investigate these schemes under the assumption of AF relaying.

Appendix A
Derivation of (26)

The PMF of the set $\mathcal{C}$ can be expressed as

$$\mathbb{P}(\mathcal{C}) = \prod_{\ell \in \mathcal{C}} \mathbb{P}(\ell \in \mathcal{C}) \prod_{j \notin \mathcal{C}} \mathbb{P}(j \notin \mathcal{C}). \tag{80}$$

Based on the definition of $\mathcal{C}$ given in (3), the probability that relay ℓ belongs to the set $\mathcal{C}$ can be computed as

$$\begin{aligned}\mathbb{P}(\ell \in \mathcal{C}) &= \mathbb{P}(I_{T_1,\ell} \geq R)\, \mathbb{P}(I_{T_2,\ell} \geq R) \\ &= \mathbb{P}\left(\gamma_{T_1,\ell} \geq 2^R - 1\right) \mathbb{P}\left(\gamma_{T_2,\ell} \geq 2^R - 1\right). \end{aligned} \tag{81}$$

Noting the fact that $\gamma_{T_1,\ell} \sim \text{Gamma}(M_1, \overline{\gamma}_{T_1,\ell})$ and $\gamma_{T_2,\ell} \sim \text{Gamma}(M_2, \overline{\gamma}_{T_2,\ell})$, (81) can be obtained as

$$\mathbb{P}(\ell \in \mathcal{C}) = \frac{\Gamma\left(M_1, \frac{2^R-1}{\overline{\gamma}_{T_1,\ell}}\right)}{\Gamma(M_1)} \times \frac{\Gamma\left(M_2, \frac{2^R-1}{\overline{\gamma}_{T_2,\ell}}\right)}{\Gamma(M_2)}. \tag{82}$$

Substituting (82) into (80), we get (26).

Appendix B
Derivation of (44)

Based on the definition of $\mathcal{C}$ given in (13), the probability that relay ℓ belongs to the set $\mathcal{C}$ can be expressed as

$$\begin{aligned}\mathbb{P}(\ell \in \mathcal{C}) &= \mathbb{P}\big((\gamma_{T_1,\ell}, \gamma_{T_2,\ell}) \in \mathcal{D}\big) \\ &\approx \mathcal{F}\left(\overline{\gamma}_{T_1,\ell}, \overline{\gamma}_{T_2,\ell}, R\right) \end{aligned} \tag{83}$$

where the region $\mathcal{D}$ is defined as $\mathcal{D} = \{\gamma_{T_1,\ell} \geq 2^R - 1,\ \gamma_{T_2,\ell} \geq 2^R - 1,\ \gamma_{T_1,\ell} + \gamma_{T_2,\ell} \geq 2^{2R} - 1\}$ and the second step follows from approximating the region $\mathcal{D}$ by $\mathcal{D}_1 \cup \mathcal{D}_2$, where $\mathcal{D}_1 = \{\gamma_{T_1,\ell} \geq 2^R - 1,\ \gamma_{T_2,\ell} \geq 2^{2R} - 2^R\}$ and $\mathcal{D}_2 = \{\gamma_{T_1,\ell} \geq 2^{2R} - 2^R,\ 2^R - 1 \leq \gamma_{T_2,\ell} < 2^{2R} - 2^R\}$. Substituting (83) into (80), we get (44).

Appendix C
Derivation of (50)

Noting the fact that $\lim_{t_2 \to 0} \Gamma(t_1, t_2) = \Gamma(t_1)$, we can write

$$\lim_{\substack{\overline{\gamma}_{T_1,\ell} \to \infty \\ \overline{\gamma}_{T_2,\ell} \to \infty}} \prod_{\ell \in \mathcal{C}} \left(\frac{\Gamma\left(M_1, \frac{2^R-1}{\overline{\gamma}_{T_1,\ell}}\right)}{\Gamma(M_1)} \times \frac{\Gamma\left(M_2, \frac{2^R-1}{\overline{\gamma}_{T_2,\ell}}\right)}{\Gamma(M_2)} \right) = 1 \tag{84}$$

$$\lim_{\substack{\overline{\gamma}_{T_1,j} \to \infty \\ \overline{\gamma}_{T_2,j} \to \infty}} \prod_{j \notin \mathcal{C}} \left(1 - \prod_{i=1}^{2} \frac{\Gamma\left(M_i, \frac{2^R-1}{\overline{\gamma}_{T_i,j}}\right)}{\Gamma(M_i)} \right) = \begin{cases} 1, & \mathcal{C} = \mathcal{P} \\ 0, & \mathcal{C} \neq \mathcal{P} \end{cases} \tag{85}$$

Letting $\overline{\gamma}_{T_1,\ell} \to \infty$ and $\overline{\gamma}_{T_2,\ell} \to \infty$ in (49) and using (84) and (85), we get (50).

This article has been accepted for publication in a future issue of this journal, but has not been fully edited. Content may change prior to final publication. Citation information: DOI 10.1109/TVT.2018.2867894, IEEE Transactions on Vehicular Technology

APPENDIX D
PROOF OF LEMMA 1

The upper incomplete gamma function can be expressed in terms of the complete gamma function as

$$\Gamma(t_1, t_2) = \Gamma(t_1) - \int_0^{t_2} x^{t_1-1} e^{-x}\, dx. \tag{86}$$

Using the Taylor's series expansion for the exponential term, (86) can be computed as

$$\Gamma(t_1, t_2) = \Gamma(t_1) - \sum_{i=0}^{\infty} \frac{(-1)^i}{(i+t_1)\, i!} (t_2)^{i+t_1}. \tag{87}$$

For the case that t_2 goes to zero, the term corresponding to $i = 0$ is the dominant term of the summation. Thus, (87) can be expressed asymptotically as (69).

ACKNOWLEDGMENT

The authors would like to thank the Associate Editor and anonymous reviewers for their very constructive comments.

REFERENCES

[1] J. N. Laneman, D. N. C. Tse, and G. W. Wornell, "Cooperative diversity in wireless networks: Efficient protocols and outage behavior," *IEEE Trans. Inf. Theory*, vol. 50, no. 12, pp. 3062–3080, Dec. 2004.

[2] T. Wang, Y. Yao, and G. B. Giannakis, "Non-coherent distributed space–time processing for multiuser cooperative transmissions," *IEEE Trans. Wireless Commun.*, vol. 5, no. 12, pp. 3339–3343, Dec. 2006.

[3] A. H. Bastami and A. Olfat, "Optimal incremental relaying in cooperative diversity systems," *IET Commun.*, vol. 7, no. 2, pp. 152–168, 2013.

[4] S. W. Kim and R. Cherukuri, "Cooperative spatial multiplexing for high-rate wireless communications," in *Proc. IEEE Workshop Signal Process. Advances in Wireless Commun.*, New York, Jun. 2005, pp. 181–185.

[5] A. H. Bastami and M. B. N. Shirazi, "Cooperative spatial multiplexing with joint incremental selective relaying," in *Proc. IWCIT*, Tehran, May 2016, pp. 1–6.

[6] A. Darmawan, S. W. Kim, and H. Morikawa, "LLR-based ordering in amplify-and-forward cooperative spatial multiplexing system," in *Proc. IEEE WCNC*, Kowloon, Mar. 2007, pp. 819–824.

[7] T. Q. Duong and H.-J. Zepernick, "Performance analysis of cooperative spatial multiplexing with amplify-and-forward relays," in *Proc. IEEE PIMRC*, Tokyo, Sep. 2009, pp. 1963–1967.

[8] N. Xie and A. Burr, "Distributed cooperative spatial multiplexing with Slepian Wolf code," in *Proc. IEEE 77th VTC*, Dresden, 2013, pp. 1–5.

[9] N. Xie and A. Burr, "Implementation of Slepian Wolf theorem in a distributed cooperative spatial multiplexing system," in *Proc. 20th European Wireless Conf.*, Barcelona, May 2014, pp. 689–693.

[10] R. Zhang, Y.-C. Liang, C. C. Chai, and S. Cui, "Optimal beamforming for two-way multi-antenna relay channel with analogue network coding," *IEEE J. Sel. Areas Commun.*, vol. 27, no. 5, pp. 699–712, Jun. 2009.

[11] Y. Wu, P. A. Chou, S. Y. Kung, "Information exchange in wireless networks with network coding and physical-layer broadcast," in *Proc. 39th Annual Conf. Inform. Sci. and Systems (CISS)*, Mar. 2005.

[12] Y. Li, R. H. Y. Louie, and B. Vucetic, "Relay selection with network coding in two-way relay channels," *IEEE Trans. Veh. Technol.*, vol. 59, no. 9, pp. 4489–4499, Nov. 2010.

[13] H. Liu, P. Popovski, E. Carvalho, and Y. Zhao, "Sum-rate optimization in a two-way relay network with buffering," *IEEE Commun. Lett.*, vol. 17, no. 1, pp. 95–98, Jan. 2013.

[14] Z. Yi, M. Ju, and I.-M. Kim, "Outage probability and optimum combining for time division broadcast protocol," *IEEE Trans. Wireless Commun.*, vol. 10, no. 5, pp. 1362–1367, May 2011.

[15] S. Yadav and P. K. Upadhyay, "Impact of outdated channel estimates on opportunistic two-way ANC-based relaying with three-phase transmissions," *IEEE Trans. Veh. Technol.*, vol. 64, no. 12, pp. 5750–5766, Dec. 2015.

[16] S. Zhang, S. C. Liew, and P. P. Lam, "Hot topic: physical layer network coding," in *Proc. 12th MobiCom*, Los Angeles, California, USA, Sept. 2006, pp. 358–365.

[17] M. Eslamifar, W. H. Chin, C. Yuen, and Y. L. Guan, "Performance analysis of two-step bi-directional relaying with multiple antennas," *IEEE Trans. Wireless Commun.*, vol. 11, no. 12, pp. 4237–4242, Dec. 2012.

[18] S. Yadav, P. K. Upadhyay, and S. Prakriya, "Performance evaluation and optimization for two-way relaying with multi-antenna sources," *IEEE Trans. Veh. Technol.*, vol. 63, no. 6, pp. 2982–2989, Jul. 2014.

[19] C. Chen, L. Bai, Y. Yang, and J. Choi, "Error performance of physical-layer network coding in multiple-antenna two-way relay systems with outdated CSI," *IEEE Trans. Commun.*, vol. 63, no. 10, pp. 3744–3753, Oct. 2015.

[20] S. Wei, J. Li, W. Chen, L. Zheng, and H. Su, "Design of generalized analog network coding for a multiple-access relay channel," *IEEE Trans. Commun.*, vol. 63, no. 1, pp. 170–185, Jan. 2015.

[21] A. H. Bastami, "Two-way incremental relaying with symbol-based network coding: performance analysis and optimal thresholds," *IEEE Trans. Commun.*, vol. 65, no. 2, pp. 564–578, Feb. 2017.

[22] H. Ding, J. Ge, D. B. da Costa, and Z. Jiang, "Two birds with one stone: exploiting direct links for multiuser two-way relaying systems," *IEEE Trans. Wireless Commun.*, vol. 11, no. 1, pp. 54–59, Jan. 2012.

[23] L. K. S. Jayasinghe, N. Rajatheva, and M. Latva-aho, "Joint pre-coder and decoder design for physical layer network coding based MIMO two-way relay system," in *Proc. IEEE ICC*, Jun. 2012, pp. 5645–5649.

[24] C. Y. Leow, Z. Ding, and K. K. Leung, "Joint beamforming and power management for non-regenerative MIMO two-way relaying channels," *IEEE Trans. Veh. Technol.*, vol. 60, no. 9, pp. 4374–4383, Nov. 2011.

[25] G. Amarasuriya, C. Tellambura, and M. Ardakani, "Sum rate analysis of two-way MIMO AF relay networks with zero-forcing," *IEEE Trans. Wireless Commun.*, vol. 12, no. 9, pp. 4456–4469, Sep. 2013.

[26] C.-L. Wang, J.-Y. Chen, and Y.-H. Peng, "Relay precoder designs for two-way amplify-and-forward MIMO relay systems: an eigenmode-selection approach," *IEEE Trans. Wireless Commun.*, vol. 15, no. 7, pp. 5127–5137, Jul. 2016.

[27] J. Guo, T. Yang, J. Yuan, and J. A. Zhang, "Linear vector physical-layer network coding for MIMO two-way relay channels: Design and performance analysis," *IEEE Trans. Commun.*, vol. 63, no. 7, pp. 2591–2604, Jul. 2015.

[28] H. M. Nguyen, V. B. Pham, X. N. Tran, and T. N. Tran, "Channel quantization based physical-layer network coding for MIMO two-way relay networks," in *Proc. IEEE Int. Conf. Advanced Technol. Commun. (ATC)*, Oct. 2016, pp. 197–203.

[29] H. Gao, X. Su, T. Lv, and Z. Zhang, "Joint relay antenna selection and zero-forcing spatial multiplexing for MIMO two-way relay with physical-layer network coding," in *Proc. IEEE GLOBECOM*, Dec. 2011, pp. 1–6.

[30] H. Park, J. Chun, and R. Adve, "Computationally efficient relay antenna selection for AF MIMO two-way relay channels," *IEEE Trans. Signal Process.*, vol. 60, no. 11, pp. 6091–6097, Nov. 2012.

[31] S. Silva, G. Amarasuriya, C. Tellambura, and M. Ardakani, "Relay selection strategies for MIMO two-way relay networks with spatial multiplexing," *IEEE Trans. Commun.*, vol. 63, no. 12, pp. 4694–4710, Dec. 2015.

[32] S. Silva, G. Amarasuriya, C. Tellambura, and M. Ardakani, "Relay selection for MIMO two-way relay networks with spatial multiplexing," in *Proc. IEEE ICCW*, London, Jun. 2015, pp. 943–948.

[33] R. Ahlswede, N. Cai, S.-Y. R. Li, and R. W. Yeung, "Network information flow," *IEEE Trans. Inf. Theory*, vol. 46, no. 4, pp. 1204–1216, Jul. 2000.

[34] L. Shi, T. Yang, K. Cai, P. Chen, and T. Guo, "On MIMO linear physical-layer network coding: Full-rate full-diversity design and optimization," *IEEE Trans. Wireless Commun.*, vol. 17, no. 5, pp. 3498–3511, May 2018.

[35] A. Goldsmith, S. A. Jafar, N. Jindal, and S. Vishwanath, "Capacity limits of MIMO channels," *IEEE J. Sel. Areas Commun.*, vol. 21, no. 5, pp. 684–702, Jun. 2003.

[36] A. Ragaleux, S. Baey, and M. Karaca, "Standard-compliant LTE-A uplink scheduling scheme with quality of service," *IEEE Trans. Veh. Technol.*, vol. 66, no. 8, pp. 7207–7222, Aug. 2017.

[37] P. G. Moschopoulos, "The distribution of the sum of independent gamma random variables," *Ann. Inst. Statist. Math.*, vol. 37, no. 1, pp. 541–544, Dec. 1985.

[38] Q. F. Zhou, F. C. M. Lau, and S. F. Hau, "Asymptotic analysis of opportunistic relaying protocols," *IEEE Trans. Wireless Commun.*, vol. 8, no. 8, pp. 3915–3920, Aug. 2009.

[39] L. Zheng and D. Tse, "Diversity and multiplexing: a fundamental tradeoff in multiple antenna channels," *IEEE Trans. Inf. Theory*, vol. 49, no. 5, pp. 1073–1096, May 2003.

[40] H. Wicaksana, S. H. Ting, Y. L. Guan, and X.-G. Xia, "Decode-and-forward two-path half-duplex relaying: Diversity-multiplexing tradeoff analysis," *IEEE Trans. Commun.*, vol. 59, no. 7, pp. 1985–1994, Jul. 2011.